SKB

TECHNICAL REPORT 91-26

Testing of parameter averaging techniques for far-field migration calculations using FARF31 with varying velocity

Akke Bengtsson[1], Anders Boghammar[1],
Bertil Grundfelt[1], Anders Rasmuson[2]

[1] Kemakta Consultants Co
[2] Chalmers Institute of Technology

June 1991

SVENSK KÄRNBRÄNSLEHANTERING AB
SWEDISH NUCLEAR FUEL AND WASTE MANAGEMENT CO

BOX 5864 S-102 48 STOCKHOLM

TEL 08-665 28 00 TELEX 13108 SKB S
TELEFAX 08-661 57 19

TESTING OF PARAMETER AVERAGING TECHNIQUES FOR FAR-FIELD MIGRATION CALCULATIONS USING FARF31 WITH VARYING VELOCITY

Akke Bengtsson[1]
Anders Boghammar[1]
Bertil Grundfelt[1]
Anders Rasmuson[2]

[1]Kemakta Consultants Co
[2]Chalmers Institute of Technology

June 1991

KEMAKTA AR 91-09

Testing of parameter averaging techniques for far-field migration calculations using FARF31 with varying velocity.

Akke Bengtsson[1]
Anders Boghammar[1]
Bertil Grundfelt[1]
Anders Rasmuson[2]

[1]KEMAKTA Consultants Co
[2]Chalmers Institute of Technology

June 19, 1991

ABSTRACT :

This report was prepared for SKB as a part of the SKB 91 performance assessment study. The object of the study was to test different averaging techniques for averaging velocity profiles. The average velocities obtained with the different techniques were used to set appropriate values on the Peclet number, Pe, and the groundwater travel time, t_w, and used as input to the FARF31 code. The output from the FARF31 calculations were compared against numerical simulations made with TRUCHN. Three different averaging techniques were tested : volume averaging, flow averaging and a technique based on the principle of additive variances. Four different nuclides were studied, ^{238}U, ^{237}Np, ^{135}Cs and ^{129}I. Five velocity profiles were tested, four generic profiles and one particle track from the groundwater flow calculations made for the Finnsjö site.

TABLE OF CONTENTS

1 BACKGROUND

The SKB 91 study is a performance assessment study for a repository for high-level radioactive waste in crystalline rock. The performance assessment makes use of a series of models describing the physical and chemical phenomena governing the release of radionuclides from the repository to the environment. This study aims at investigating various techniques for averaging model parameters for the radionuclide transport through the far field.

The far-field transport will in SKB 91 be modelled as transport through a set of flow tubes. These are defined from the results of a groundwater flow model by using particle tracking to evaluate the flow lines and the flow rate distribution along the flow lines. The conceptual model used for the transport includes advective and dispersive transport in fractures in the rock coupled with diffusion into micropores in the adjacent rock matrix.

According to plans, the FARF31 code *[S.Norman, N.Kjellbert, 1990]* will be used to calculate the radionuclide transport along the flow tubes. This code is based on an analytical solution in the Laplace plane of the transport equations. The Laplace-transformed equations are then numerically inverted using the Talbot algorithm. The code requires that the parameters are constant along the migration path. The groundwater velocity will, however, vary within a few orders of magnitude along the particle tracks defining the flow tubes. In order to be able to use FARF31, one therefore has to apply some averaging procedure to the flow tubes to obtain "equivalent" constant parameters.

In this study three different averaging schemes for the velocity and the dispersivity are evaluated. All other parameters are assumed to be truly constant throughout the domain. The evaluation is done for five test cases that differ in the velocity profiles along the flow tube. Four of the cases are generic whereas the fifth case is a realistic particle track taken from the finite-element modelling of the groundwater flow at the Finnsjön site in Sweden *[B.Lindbom et al, 1991]*. First the transport through the flow tube is modelled numerically using the TRUCHN code. The average parameters are then calculated and the transport modelled using the FARF31 code and the average parameters.

2 AVERAGING VELOCITIES

The model used to describe the radionuclide transport through the far field comprises advective and dispersive transport in fractures in the rock coupled with diffusion into micropores in the rock matrix adjacent to the fractures. A majority of the radionuclides interact chemically and physically (sorption) with the rock surfaces such that they move at a lower velocity than the flowing groundwater. This conceptual model is implemented through the following set of equations:

$$\frac{\partial c_i}{\partial t} = -u \frac{\partial c_i}{\partial z} + u \frac{\partial}{\partial z} \frac{D_L}{u} \frac{\partial c_i}{\partial z} - w_i - \lambda_i c_i + \lambda_{i-1} c_{i-1} \qquad (2:1)$$

$$D_e \frac{\partial^2}{\partial x^2} c_{p,i}(z,x,t) - \lambda_i R_i c_{p,i}(z,x,t) + \lambda_{i-1} R_{i-1} c_{p,i-1}(z,x,t) = R_i \frac{\partial}{\partial t} c_{p,i}(z,x,t) \qquad (2:2)$$

$$w_i(z) = -a(z) D_e \frac{\partial}{\partial x} c_{p,i}(z,x,t) \Big|_{x=0} \qquad (2:3)$$

These equations contain the following main parameters:

- Parameters governing the advective transport: **u**
- Parameters governing dispersion: $\mathbf{D_L}$
- Parameters governing diffusion into the rock matrix: **a**, $\mathbf{D_e}$
- Parameters governing sorption: **R**
- Parameters governing radiactive decay: λ

In this study all parameters except the groundwater velocity and the dispersion coefficient (actually the Peclet number, $P_e=L \cdot u/D_L$) are assumed to be constant along the migration path. The reason for this is simply that there is no evidence to support any specific mode of variation of the other parameters. This chapter outlines the different techniques used in this study to average velocities. Three different types of averaging techniques have been studied :

- Volume average
- Flow average
- Averaging using the additive variance approach

The first two techniques aim at averaging the velocity in the advective term of Equation 2:1, while the Peclet number is given a value estimated prior to the exercise. In the third approach an average velocity to be used in the Peclet number is calculated while the velocity in the advective term is taken as the volume average. These averaging techniques are described below.

2.1 VOLUME AVERAGE

The volume-averaged velocity is calculated by applying the formulae :

$$t_w = \int_0^L \frac{dx}{u(x)} \tag{2:4}$$

$$\bar{u} = \frac{L}{t_w} = \frac{L}{\int_0^L \frac{dx}{u(x)}} \tag{2:5}$$

The Peclet number is set to a prior estimate. The Peclet number is :

$$P_e = \frac{\bar{u}\, L}{D_L} \tag{2:6}$$

This form is the most straightforward way of formulating average velocities. It will correctly focus on the primary variable for matrix diffusion: the contact time. However, dispersive effects will be underestimated. For the case of no dispersion the problem is analytically solvable with arbitrary u(x).

2.2 FLOW AVERAGE

The flow-averaged velocity is calculated using the formulae :

$$\bar{u} = \frac{1}{L} \int_0^L u(x)dx \tag{2:7}$$

The residence time input to the FARF31 code, is calculated by applying Equation 2:5 with the average velocity calculated from Equation 2:7.

$$t_w^* = \frac{L}{\bar{u}} = \frac{L}{\frac{1}{L}\int_0^L u(x)dx} \tag{2:8}$$

The Peclet number is set to a prior estimate.

This technique of averaging velocities emphasizes the high-velocity parts of the stream tube. Since the transport in these parts is mainly governed by the advective transport, this type of averaging may not be physically representative, and it will certainly underestimate matrix diffusion effects.

2.3 ADDITIVE VARIANCES

This approach is based on the use of different average velocities in the Peclet number and in the advective term In the advecti"e term a volume-averaged velocity is used (Equations 2:4 and 2:5). The average velocity used in the Peclet number is calculated using *[Neretnieks and Rasmuson, 1984]* :

$$\bar{u} = \frac{t_w}{\int_0^L \frac{dx}{u(x)^2}} \qquad (2:9)$$

The Peclet number is calculated using:

$$P_e^* = \frac{t_w \bar{u}}{\alpha} \quad where \quad \alpha = \frac{L}{P_e} \qquad (2:10)$$

where t_w is the "true" residence time (Equation 2:4) and P_e is the prior estimate of the Peclet number. The above formulae are strictly valid for small dispersions. In practice, however, it has been shown that they may also be used for problems involving larger dispersion.

2.4 SUMMARY

Figure 2.1 shows a velocity profile taken from the semi-regional Finnsjö hydrology calculations [SKB AR 90-16]. The three types of averaging that has been presented above are indicated in the figure. As can be seen the flow average does exaggerate the high-velocity part. The calculated Peclet number for the additive variance is 0.78 if the prior estimate is 2.

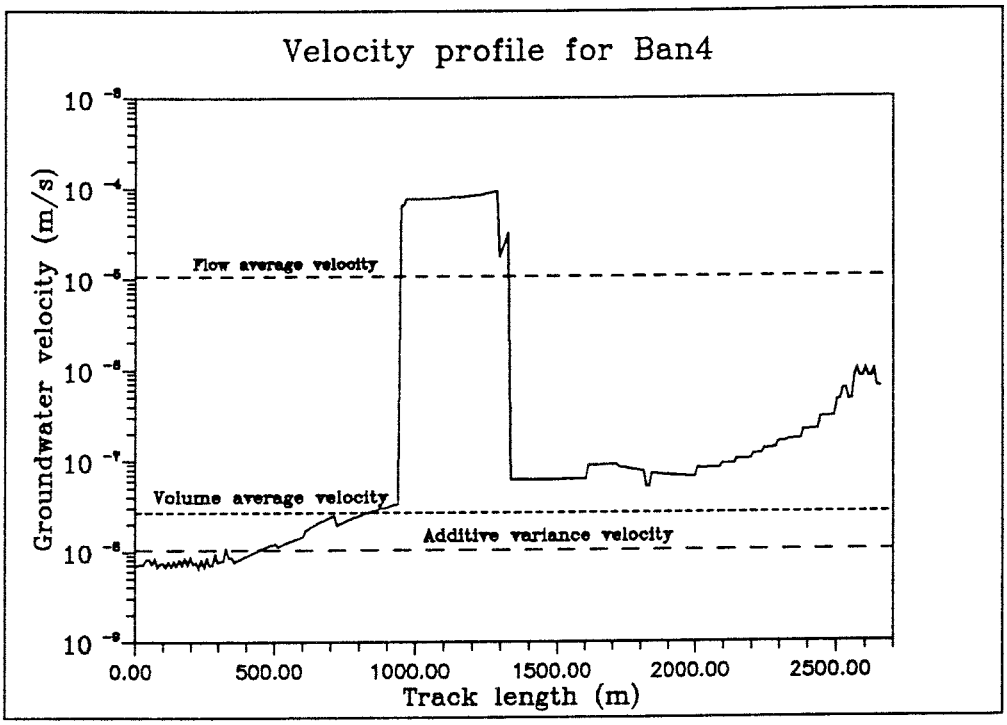

Figure 2.1 : Velocity profile for particle track number 4 from the Finnsjö area

Even though flow averaging could be shown a priori to overestimate the velocity it has been included in this study so that its effect can be demonstrated. Hence, three different parameters have been calculated for each velocity variation, these are :

t_w **according to equation 2:4**

t_w^* **according to equation 2:8**

P_e^* **according to equation 2:10**

3 TEST CASE DESCRIPTION

The following chapter describes the input data used for the migration calculations. Section 3.1 describes the general input data used for the different nuclides and the host rock. In Section 3.2 the four generic test cases are described, and finally in Section 3.3 the Finnsjö test case is presented.

3.1 GENERAL DESCRIPTION

3.1.1 Nuclide specific data

The four different nuclides that have been studied are : ^{238}U, ^{237}Np, ^{135}Cs and ^{129}I. Table 3.1 shows the data used for these nuclides *([KBS 3, 1983]* and *[B.Allard et al]*).

Table 3.1 : Nuclide specific data used in migration calculations.

Nuclide	K_d [m^3/kg]	D_a [m^2/a]	Mass	$T_{1/2}$ [a]	λ [1/a]
^{238}U	2	$2.92785 \cdot 10^{-10}$	238	$4.468 \cdot 10^{9}$	$1.55136 \cdot 10^{-10}$
^{237}Np	2	$2.92785 \cdot 10^{-10}$	237	$2.140 \cdot 10^{6}$	$3.23901 \cdot 10^{-7}$
^{135}Cs	0.03	$1.95186 \cdot 10^{-8}$	135	$3.000 \cdot 10^{6}$	$2.31049 \cdot 10^{-7}$
^{129}I	0	$7.88940 \cdot 10^{-4}$	129	$1.600 \cdot 10^{7}$	$4.33217 \cdot 10^{-8}$

The source term used for the four different nuclides is shown in Figure 3.1. The source term used for ^{238}U and ^{237}Np were constant band inputs whereas for ^{135}Cs and ^{129}I decaying band inputs were used.

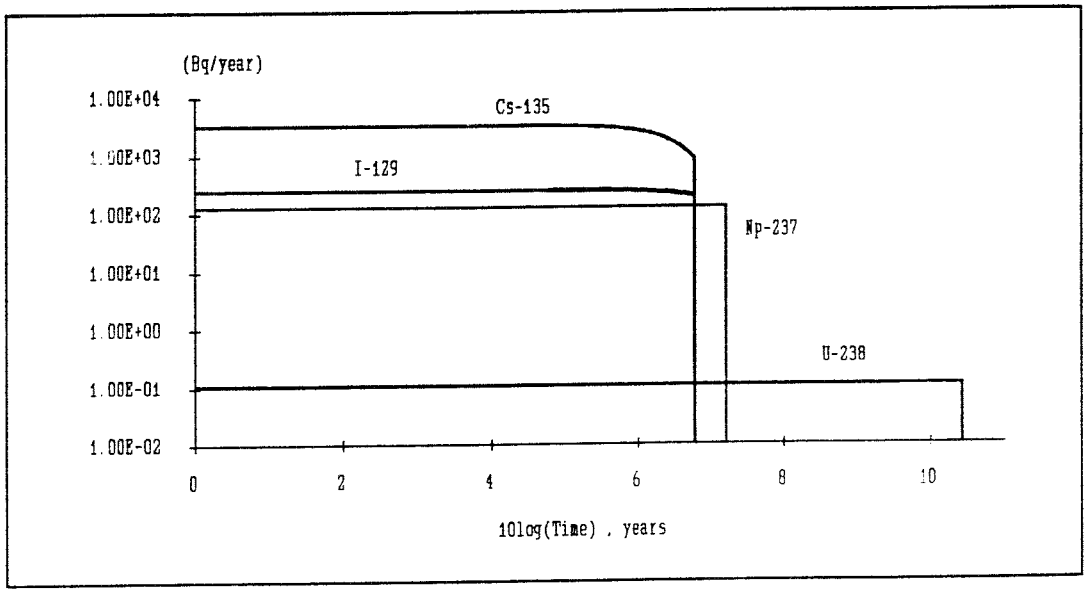

Figure 3.1 : Input time series for the four different nuclides used in the migration calculations with TRUCHN and FARF31.

3.1.2 Host rock and fluid specific data

Table 3.2 shows the data used describing the host rock and fluid environment.

***Table 3.2** : Host rock and fluid specific data.*

Variable	Value	Unit	Used in FARF31
ε_f	0.0001		
ε_p	0.002		EPSP
D_e	$1.5778 \cdot 10^{-6}$	[m^2/a]	DEFF
ρ_p	2700	[kg/m^3]	
S	5	[m]	DEPTH*2
2B	0.0005	[m]	
a	4000.0	[1/m]	ASPEC

The prior estimate of the Peclet number is assumed to be 2 *[KBS 3, 1983]*.

3.2 GENERIC TEST CASES

The generic test cases that will be outlined in the subsequent sections, were designed to test the effect of the different types of averaging technique used on different types of velocity changes. The four generic cases designed are : linearly increasing, exponentially increasing, piecewise constant and sinusoidally varying velocity. The four cases were all designed with the same stream tube length, 500 metres and an average (volume average) velocity of 1 m/a. Figure 3.2 shows the four velocity profiles. It should be noted that, although the volume average velocity is the same in all the test cases, the maximum velocity is significantly lower in the linear and the sinusiodal cases than in the other two cases.

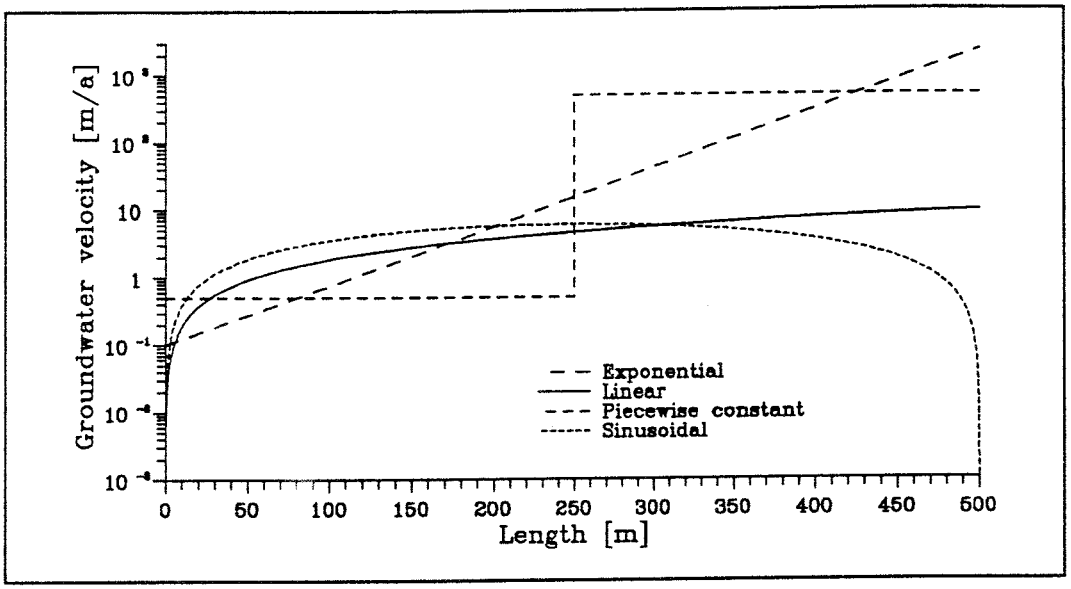

Figure 3.2 : Velocity variation along stream tube for the four generic test cases. (Note that the scale is logarithmic on the ordinate axis.)

3.2.1 Linearly increasing velocity

The formula used for the linearly increasing velocity variation is :

$$u_0 = \alpha + \beta \cdot x \qquad (3:1)$$

where α is $1.0 \cdot 10^{-7}$ and β is $1.82 \cdot 10^{-6}$.
The three parameters for the average technique testing is calculated to :

t_w : 500.0 t_w^* : 109.63 R_e^* : 0.018

3.2.2 Exponentially increasing velocity

The formula used for the exponentially increasing velocity is :

$$u_0 = \alpha \cdot e^{(\beta \cdot x)} \tag{3:2}$$

where α was set to $9.99 \cdot 10^{-6}$ and β was set to $2.0 \cdot 10^{-2}$.
The three parameters for the average technique testing is calculated to :

t_w : 500.0 t_w^* : 1.315 P_e^* : 0.399

3.2.3 Piecewise constant velocity

The formula used for the piecewise constant velocity variation is :

$$\begin{aligned} u_0 &= \alpha \qquad x \le 250 \\ u_0 &= \beta \qquad x > 250 \end{aligned} \tag{3:3}$$

where α was set to $5.00501 \cdot 10^{-5}$ and β was set to $5.000 \cdot 10^{-2}$
The three parameters for the average technique testing is calculated to :

t_w : 500.0 t_w^* : 1.998 P_e^* : 1.002

3.2.4 Sinusoidally varying velocity

The formula used for the sinusoidally varying velocity is :

$$u_0 = \alpha + \beta \cdot \sin\left(\pi \cdot \frac{x}{L}\right) \tag{3:4}$$

where α was set to $1.00 \cdot 10^{-7}$ and β was set to $5.974 \cdot 10^{-4}$
The three parameters for the average technique testing is calculated to :

t_w : 500.0 t_w^* : 131.76 P_e^* : 0.019

3.3 THE FINNSJÖ TEST CASE

One "real" test case has been choosen. It has been taken from the groundwater flow calculations performed with the NAMMU code on the Finnsjö area [SKB AR 90-16]. Within that project eight different particle tracks where computed. Particle track number four has been choosen since it had the smothest velocity profile of the eight tracks.

Figure 2.1 shows the velocity profile. The three parameters for the average technique testing is calculated to :

t_w : 3126.0 t_w^* : 7.71 P_e^* : 0.78

3.4 SUMMARY OF TEST CASES

The evaluated "averaged" parameters are summarized in Table 3.3. It is worth noting that the flow averaged residence time is extremely short in the test cases in which the velocity is high in a part of the domain. In the test case with a predominantly low velocity the Peclet number evaluated from the additive variance principle is low.

Table 3.3 : Averaged parameter values.

Test case	t_w	t_w^*	P_e^*
Linear increase	500.0	109.65	0.018
Exponential increase	500.0	1.315	0.399
Piecewise constant	500.0	1.998	1.002
Sinusiodal variation	500.0	131.76	0.019
Finnsjö test case	3126.0	7.71	0.78

4 EVALUATION OF AVERAGING STRATEGIES

Chapter 4 presents the calculations performed within this project. Section 4.1 presents a general description of the two codes used. In Section 4.2 a comparison is made between the reference calculations made with the TRUCHN code and the analytical results obtained with the FARF31 code. In addition Section 4.3 presents the effect of assuming a different Pe number.

4.1 NUMERICAL MODELLING

4.1.1 TRUCHN

For the numerical reference calculations the Integrated Finite Differences (IFD) code TRUCHN has been used *[A.Rasmuson et al, 1982]*. With the help of the preprocessing code PRETRU *[A.Bengtsson, 1990]* a discretisation has been made for each of the five different flow tube scenarios. The guidelines for the discretisation have been to have at least twenty nodes along the fracture from start up to the point past which the nuclide flux is to be calculated - the observation point. After the observation point at least ten more nodes are laid out to simulate a semiinfinite boundary condition. The distance into the rock matrix is discretised into twenty parts up to the observation point and ten points thereafter.

A layer of the rock matrix closest to the fracture is assumed to be in sorption- and diffusion equilibrium with the fracture and the capacity of it is included in the corresponding fracture nodes. The thickness of the layer has been chosen so that it would be fully penetrated well before nuclide breakthrough at the observation point. The reason for doing so is to avoid the very short time constants for the pure fracture nodes and as a consequence of that large number of nodes into the matrix with the only effect of dramatical increase in the calculation time.

The dispersivity for the individual nodes has been calculated in the following way. A dispersion length α is calculated from the global Peclèt number and the distance from start to the observation point as:

$$\alpha = \frac{D}{u} = l \cdot \frac{D}{ul} = \frac{l}{Pe}$$

The local ratio of dispersivity to velocity is then assumed to have the value of α everywhere along the flow tube. This particular choice of strategy for assigning local dispersivity can theoretically be shown to be correct for some simple water flow geometries while there are cases where no correlation between any local parameter values and the local dispersivity exists. The concept of a local dispersivity is altogether debated for fractured crystalline rock.

The nuclide flux past an observation point inside a TRUCHN node net is not calculated by TRUCHN but has to be calculated afterwards. In the present work it has been done using a simple UNIX shell script reading the TRUCHN main output data file and calculating the convective and dispersive nuclide flux. Regarding the shellscript and file handling, see appendix A.
The nuclide flux past the observation point could be expressed as:

$$\dot{N} = Q \cdot C - D \cdot A \cdot \frac{\partial C}{\partial x}$$

Assuming that the concentration at a point x along the fracture can be calculated by linear interpolation between the node points on each side it can be written as:

$$C = C_1 + \frac{(x - x_1)(C_2 - C_1)}{(x_2 - x_1)}$$

where index 1 and 2 stand for the fracture node points on each side of x.
Then the nuclide flux past x could be expressed as:

$$\dot{N} = Q\left[C_1 + \frac{(x - x_1)(C_2 - C_1)}{(x_2 - x_1)}\right] - D \cdot A \cdot \frac{(C_2 - c_1)}{(x_2 - x_1)}$$

4.1.2 FARF31

The FARF31 code used in the present calculations was a stand-alone version provided by SKB in executable format. The input data was provided using three different files. The standard input was used to provide the input from the near field. This was provided as time series of the nuclide fluxes. The input file "parameters" provided rock and transport parameters and the input file "chains" provided information on the nuclide chains used. For a thorough description of the FARF31 code, see *[S.Norman, N.Kjellbert, 1990]*.

As pointed out in Chapter 2, the two parameters of interest are the Peclet number, Pe, and the residence time, t_w. The rest of the input data to the FARF31 code were the same for all calculations. Chapter 3.1 shows the input data used. The input time series are also plotted in Chapter 3.1.

Some very small and simple FORTRAN codes have been programmed to facilitate the handling of all data, both input and output. The code PREFARF gets Pe number and t_w from the users, reads other input data necessary from two database files and creates the input files for a particular calculation. The POSTFARF code reads the output time series of the migration rate, divides the timeseries into a set of files, one for each nuclide, and outputs the release rate in Bq/a. In addition POSTFARF calculates the peak and integrated release for each nuclide (see Appendix A).

4.2 RESULTS

The following sections describe both the analytical migration calculations made with a stand-alone version of the FARF31 code and the numerically derived results using the TRUCHN code.

4.2.1 General result presentation

In the following presentation of the results, breakthrough curves for the parent nuclides are presented for each chain together with tables showing peak release rates and integrated released.

Using volume averaged velocity results in the same residence time for all cases except for the Finnsjö case. Hence, results using volume average velocity have only been calculated for the linearly increasing velocity case, Case A, and the Finnsjö case, Case E. For clarity the results from the volume average calculations with linearly increasing velocity have been included in the tables and plots for the other three generic test cases.

To ensure that the FARF31 and the TRUCHN codes give compatible results, TRUCHN runs were made with a constant velocity corresponding to Pe=2 and t_w=500 a. Figure 4.0 shows the results compared with FARF31 calcualtions using the same parameters. The figure is a strong indication that the migration can be calculated with a high-enough accuracy with both codes.

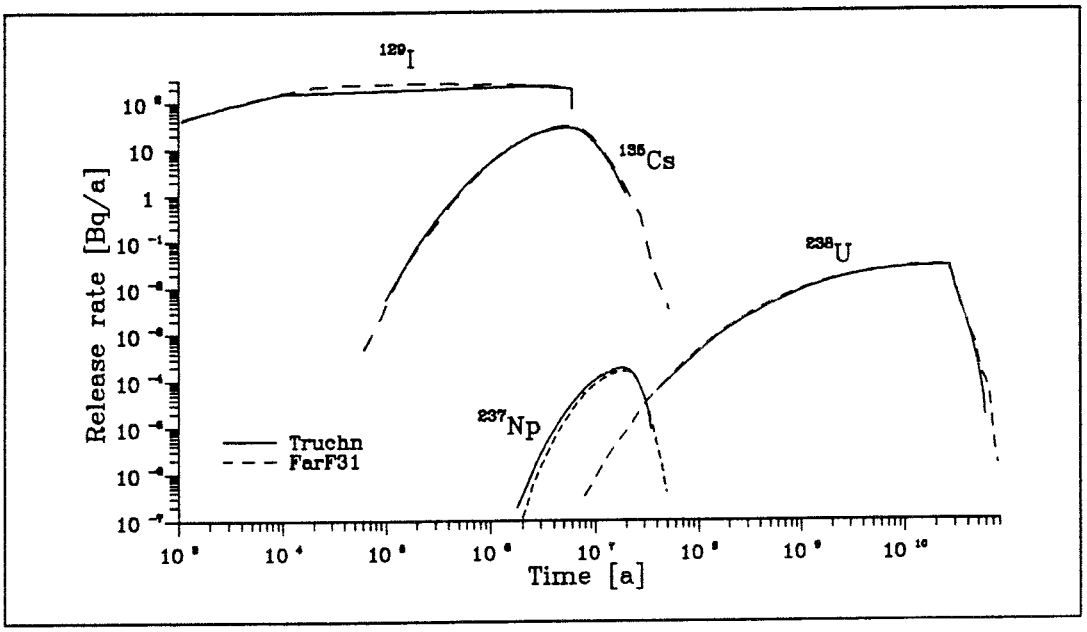

Figure 4.0 : Comparing TRUCHN results using constant velocity with FARF31 results.

4.2.2 Linearly increasing velocity

The following values were used for the three average variations performed :

Volume average :	Pe = 2	t_w = 500
Flow average :	Pe = 2	t_w = 109.6
Additive variance :	Pe = 0.018	t_w = 500

The calculated breakthrough curves are shown in Figures 4.1 - 4.4. In Table 4.1 the time of the peak release, the peak release and the integrated release are given.

Table 4.1 : Summary of release data for linearly increasing velocity.

	Volume Average	Flow Average	Additive variance	TRUCHN
^{238}U				
Peak time	$2.29 \cdot 10^{10}$	$2.47 \cdot 10^{10}$	$1.82 \cdot 10^{10}$	$2.70 \cdot 10^{10}$
Peak release	$2.88 \cdot 10^{-2}$	$7.24 \cdot 10^{-2}$	$8.69 \cdot 10^{-2}$	$2.73 \cdot 10^{-2}$
Integrated release	$7.80 \cdot 10^{8}$	$1.96 \cdot 10^{9}$	$2.43 \cdot 10^{9}$	$7.37 \cdot 10^{8}$
^{237}Np				
Peak time	$1.94 \cdot 10^{7}$	$1.65 \cdot 10^{7}$	$1.55 \cdot 10^{7}$	$1.90 \cdot 10^{7}$
Peak release	$1.58 \cdot 10^{-4}$	$3.65 \cdot 10^{-1}$	$3.16 \cdot 10^{1}$	$6.62 \cdot 10^{-4}$
Integrated release	$2.77 \cdot 10^{3}$	$5.95 \cdot 10^{6}$	$5.08 \cdot 10^{8}$	$1.13 \cdot 10^{4}$
^{135}Cs				
Peak time	$5.31 \cdot 10^{6}$	$2.59 \cdot 10^{6}$	$6.09 \cdot 10^{5}$	$4.60 \cdot 10^{6}$
Peak release	$3.03 \cdot 10^{1}$	$4.34 \cdot 10^{2}$	$1.60 \cdot 10^{3}$	$3.61 \cdot 10^{1}$
Integrated release	$2.68 \cdot 10^{8}$	$2.95 \cdot 10^{9}$	$7.36 \cdot 10^{9}$	$2.94 \cdot 10^{8}$
^{129}I				
Peak time	$1.56 \cdot 10^{5}$	$2.55 \cdot 10^{5}$	$3.57 \cdot 10^{4}$	$1.00 \cdot 10^{5}$
Peak release	$2.56 \cdot 10^{2}$	$2.52 \cdot 10^{2}$	$2.42 \cdot 10^{2}$	$2.49 \cdot 10^{2}$
Integrated release	$1.28 \cdot 10^{9}$	$1.25 \cdot 10^{9}$	$1.20 \cdot 10^{9}$	$1.31 \cdot 10^{9}$

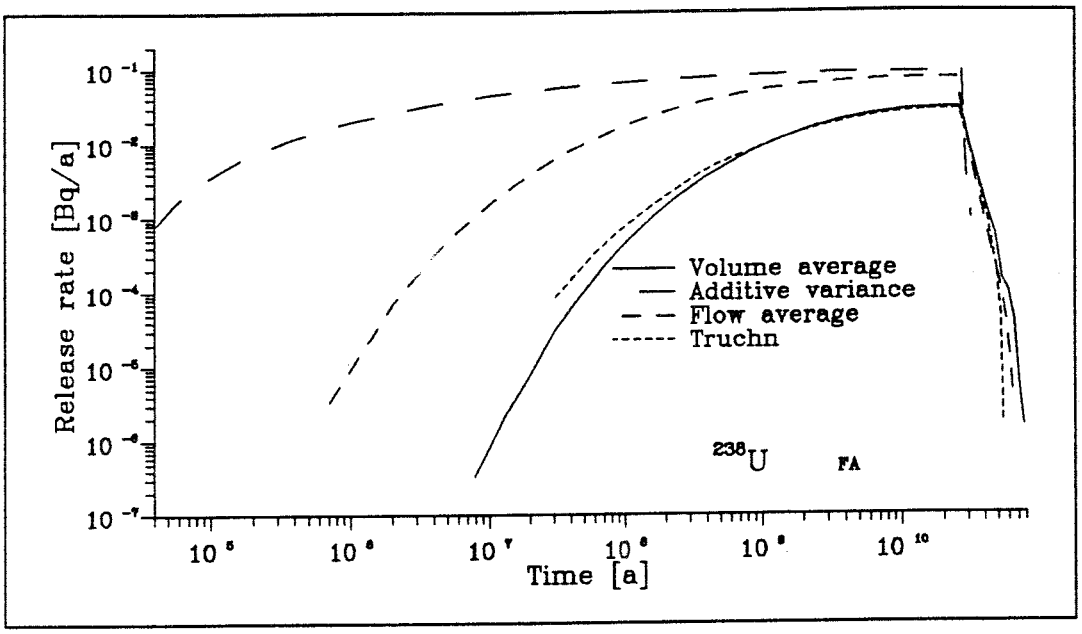

Figure 4.1 : Breakthrough for ^{238}U using linearly varying velocity.

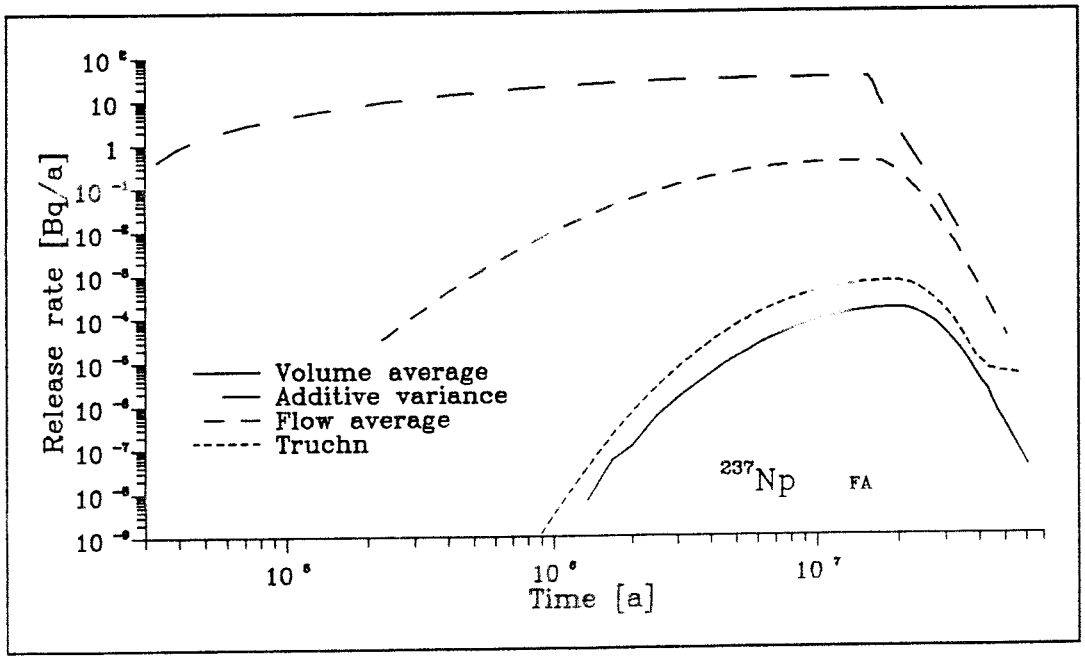

Figure 4.2 : Breakthrough for ^{237}Np using linearly varying velocity.

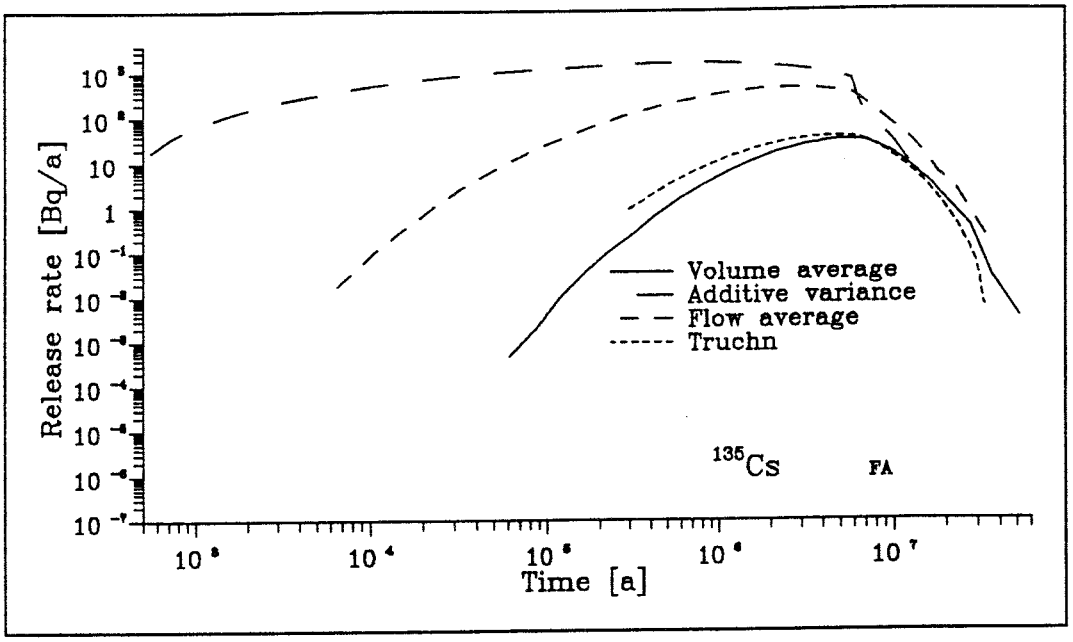

Figure 4.3 : *Breakthrough for ^{135}Cs using linearly varying velocity.*

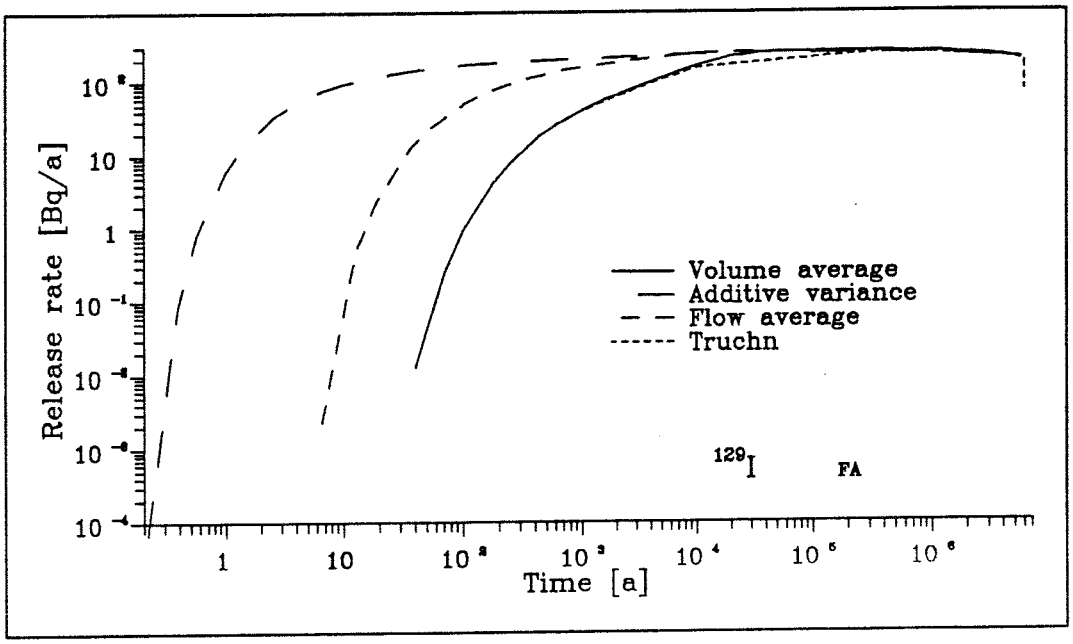

Figure 4.4 : *Breakthrough for ^{129}I using linearly varying velocity.*

4.2.3 Exponentially increasing velocity

The following values were used for the two average variations performed :

Flow average :	Pe = 2	t_w = 1.315
Additive variance :	Pe = 0.399	t_w = 500

The calculated breakthrough curves are shown in Figures 4.5 - 4.8. In Table 4.2 the time of the peak release, the peak release and the integrated release are given. The results given for volume average are identical to those shown in Section 4.2.2.

Table 4.2 : Summary of release data for exponentially increasing velocity.

	Volume average	Flow average	Additive variance	TRUCHN
^{238}U				
Peak time	$2.29 \cdot 10^{10}$	$1.97 \cdot 10^{10}$	$2.61 \cdot 10^{10}$	$2.70 \cdot 10^{10}$
Peak release	$2.88 \cdot 10^{-2}$	$1.06 \cdot 10^{-1}$	$5.08 \cdot 10^{-2}$	$6.46 \cdot 10^{-3}$
Integrated release	$7.80 \cdot 10^{8}$	$2.60 \cdot 10^{9}$	$1.37 \cdot 10^{9}$	$1.79 \cdot 10^{8}$
^{237}Np				
Peak time	$1.94 \cdot 10^{7}$	$1.06 \cdot 10^{7}$	$1.64 \cdot 10^{7}$	$1.70 \cdot 10^{7}$
Peak release	$1.58 \cdot 10^{-4}$	$1.02 \cdot 10^{2}$	$2.42 \cdot 10^{-1}$	$1.82 \cdot 10^{-2}$
Integrated release	$2.77 \cdot 10^{3}$	$1.70 \cdot 10^{9}$	$3.93 \cdot 10^{6}$	$2.96 \cdot 10^{5}$
^{135}Cs				
Peak time	$5.31 \cdot 10^{6}$	$2.04 \cdot 10^{5}$	$3.01 \cdot 10^{6}$	$6.00 \cdot 10^{6}$
Peak release	$3.03 \cdot 10^{1}$	$3.02 \cdot 10^{3}$	$2.77 \cdot 10^{2}$	$6.04 \cdot 10^{1}$
Integrated release	$2.68 \cdot 10^{8}$	$1.07 \cdot 10^{10}$	$1.89 \cdot 10^{9}$	$4.91 \cdot 10^{8}$
^{129}I				
Peak time	$1.56 \cdot 10^{5}$	$3.87 \cdot 10^{2}$	$2.42 \cdot 10^{5}$	$8.99 \cdot 10^{4}$
Peak release	$2.56 \cdot 10^{2}$	$2.43 \cdot 10^{2}$	$2.54 \cdot 10^{2}$	$2.47 \cdot 10^{2}$
Integrated release	$1.28 \cdot 10^{9}$	$1.15 \cdot 10^{9}$	$1.51 \cdot 10^{9}$	$1.40 \cdot 10^{9}$

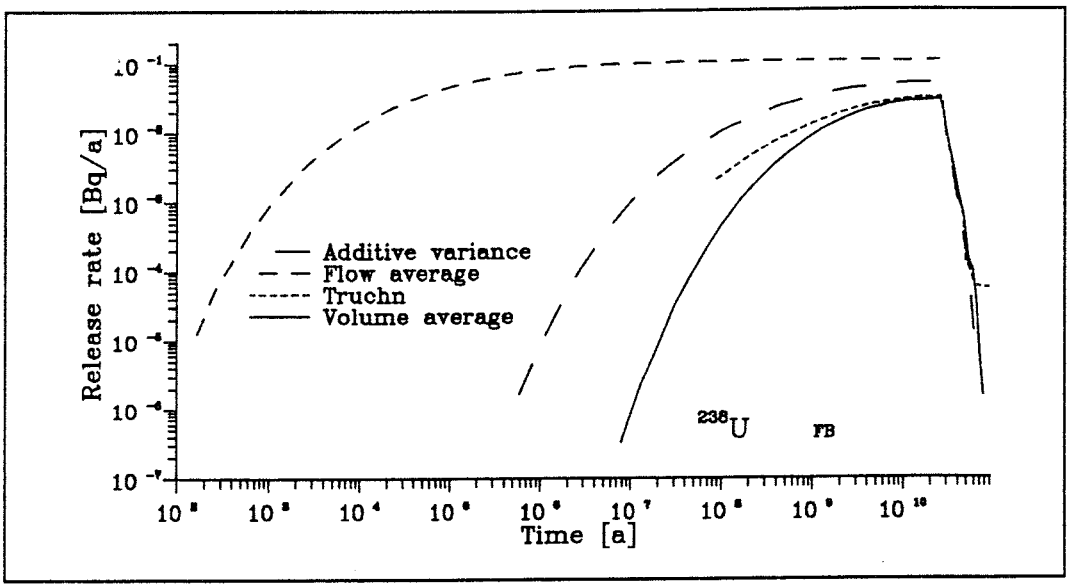

Figure 4.5 : Breakthrough for ^{238}U using exponentially increasing velocity.

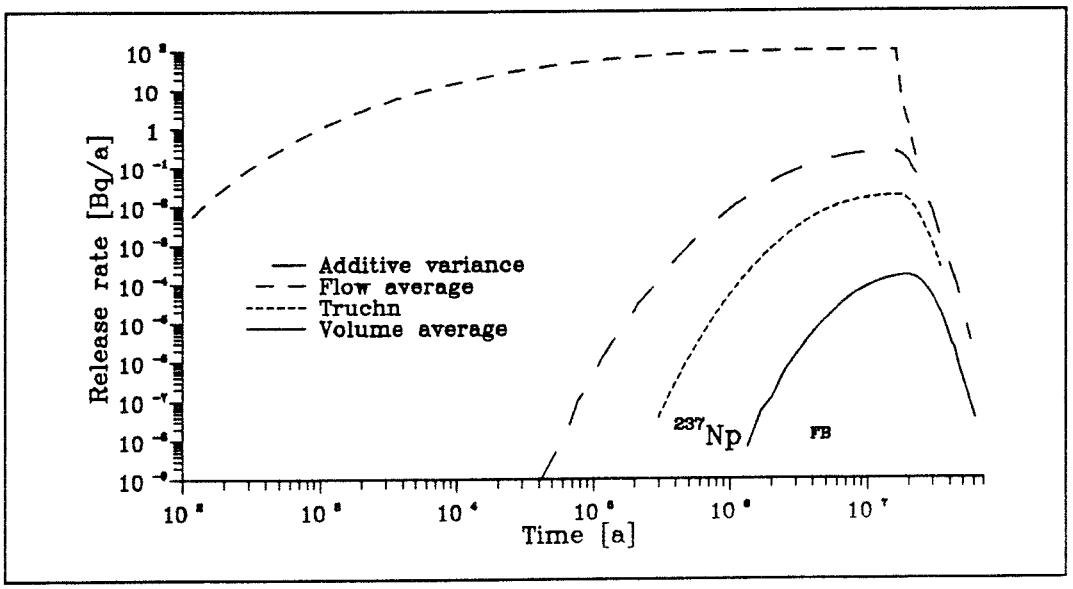

Figure 4.6 : Breakthrough for ^{237}Np using exponentially increasing velocity.

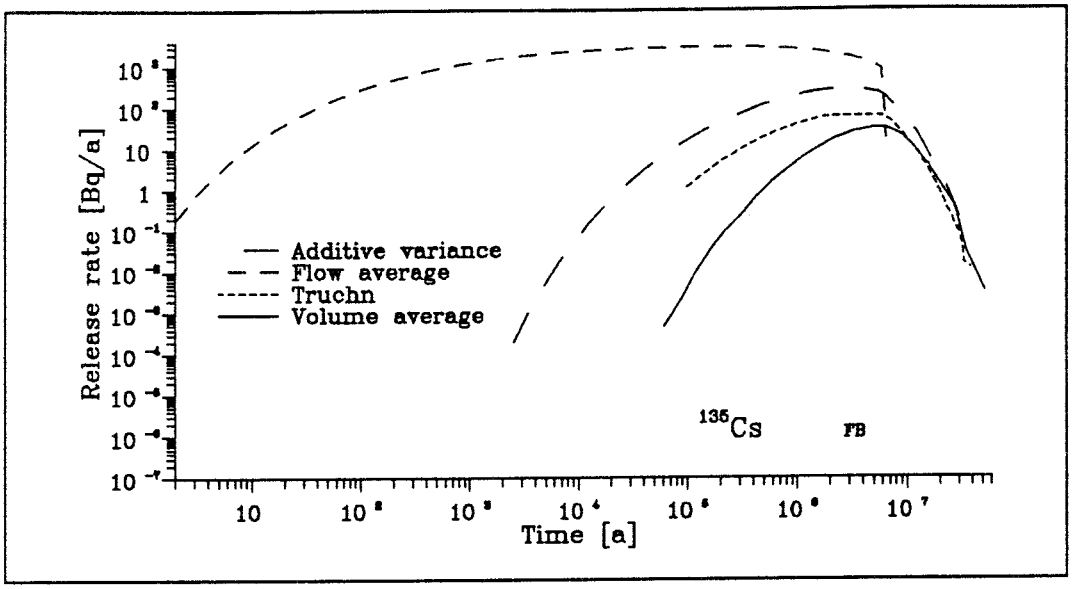

Figure 4.7 : Breakthrough for ^{135}Cs using exponentially increasing velocity.

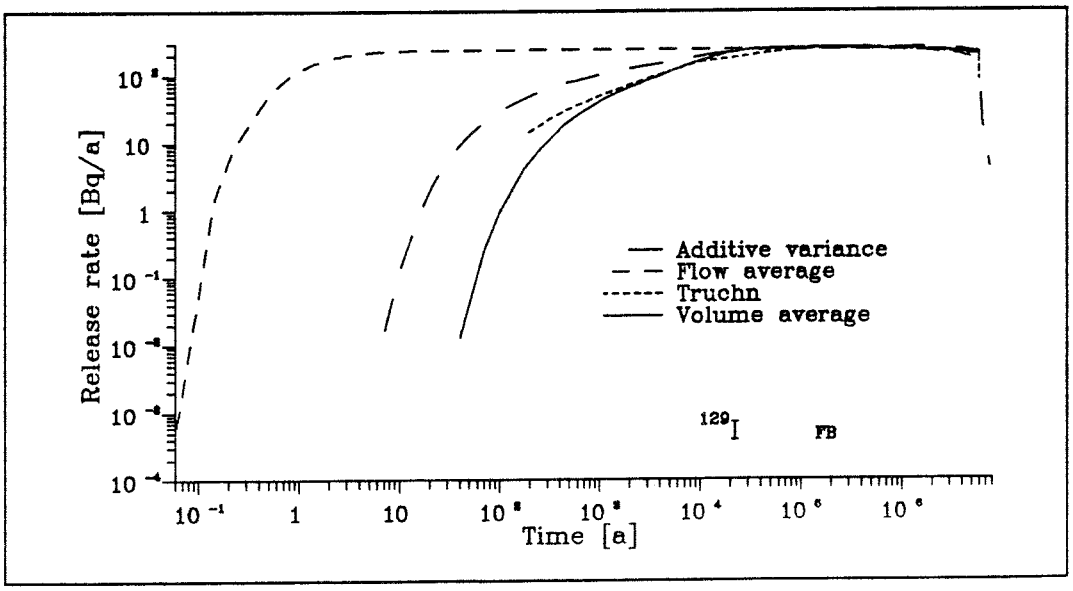

Figure 4.8 : Breakthrough for ^{129}I using exponentially increasing velocity.

4.2.4 Piecewise constant velocity

The following values were used for the two average variations performed :

Flow average :	Pe = 2	t_w = 1.998
Additive variance :	Pe = 1.002	t_w = 500

The calculated breakthrough curves are shown in Figures 4.9 - 4.12. In Table 4.3 the time of the peak release, the peak release and the integrated release are given. The results given for volume average are identical to those shown in Section 4.2.2.

Table 4.3 : Summary of release data for piecewice constant velocity.

	Volume average	Flow average	Additive variance	TRUCHN
^{238}U				
Peak time	$2.29 \cdot 10^{10}$	$9.93 \cdot 10^{9}$	$2.00 \cdot 10^{10}$	$2.70 \cdot 10^{10}$
Peak release	$2.88 \cdot 10^{-2}$	$1.04 \cdot 10^{-1}$	$3.74 \cdot 10^{-2}$	$2.76 \cdot 10^{-2}$
Integrated release	$7.80 \cdot 10^{8}$	$2.58 \cdot 10^{9}$	$1.04 \cdot 10^{9}$	$7.49 \cdot 10^{8}$
^{237}Np				
Peak time	$1.94 \cdot 10^{7}$	$1.39 \cdot 10^{7}$	$1.76 \cdot 10^{7}$	$1.80 \cdot 10^{7}$
Peak release	$1.58 \cdot 10^{-4}$	$9.17 \cdot 10^{1}$	$7.11 \cdot 10^{-3}$	$1.22 \cdot 10^{-3}$
Integrated release	$2.77 \cdot 10^{3}$	$1.52 \cdot 10^{9}$	$1.20 \cdot 10^{5}$	$2.06 \cdot 10^{4}$
^{135}Cs				
Peak time	$5.31 \cdot 10^{6}$	$2.57 \cdot 10^{5}$	$4.48 \cdot 10^{6}$	$4.60 \cdot 10^{6}$
Peak release	$3.03 \cdot 10^{1}$	$2.90 \cdot 10^{3}$	$9.00 \cdot 10^{1}$	$3.55 \cdot 10^{1}$
Integrated release	$2.68 \cdot 10^{8}$	$1.06 \cdot 10^{10}$	$7.25 \cdot 10^{8}$	$2.92 \cdot 10^{8}$
^{129}I				
Peak time	$1.56 \cdot 10^{5}$	$1.67 \cdot 10^{3}$	$5.52 \cdot 10^{6}$	$2.00 \cdot 10^{5}$
Peak release	$2.56 \cdot 10^{2}$	$2.43 \cdot 10^{2}$	$3.82 \cdot 10^{2}$	$2.47 \cdot 10^{2}$
Integrated release	$1.28 \cdot 10^{9}$	$1.17 \cdot 10^{9}$	$2.47 \cdot 10^{9}$	$1.48 \cdot 10^{9}$

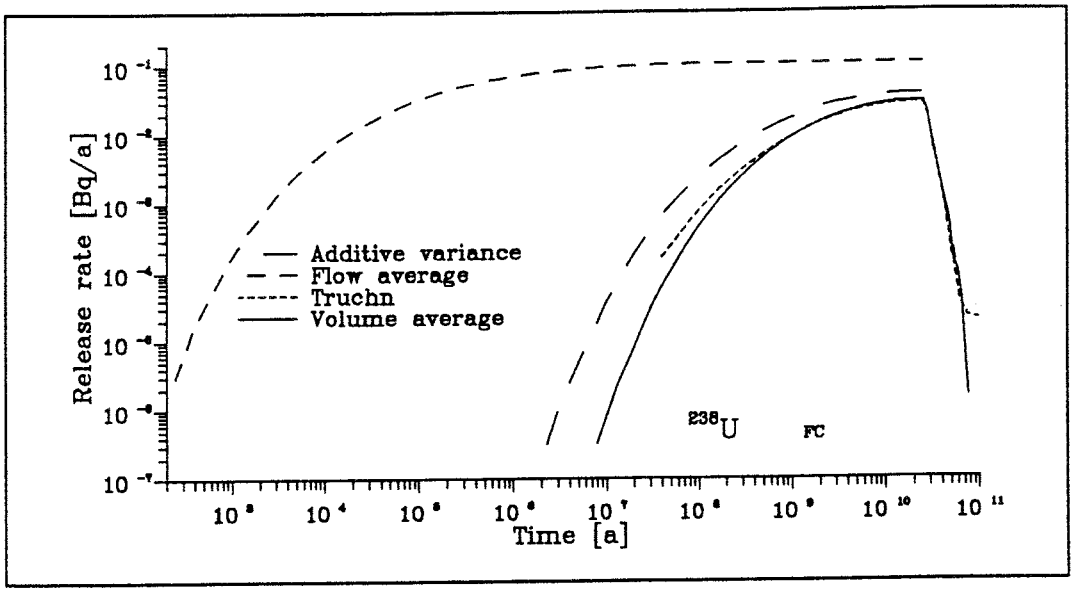

Figure 4.9 : Breakthrough for ^{238}U using piecewise constant velocity.

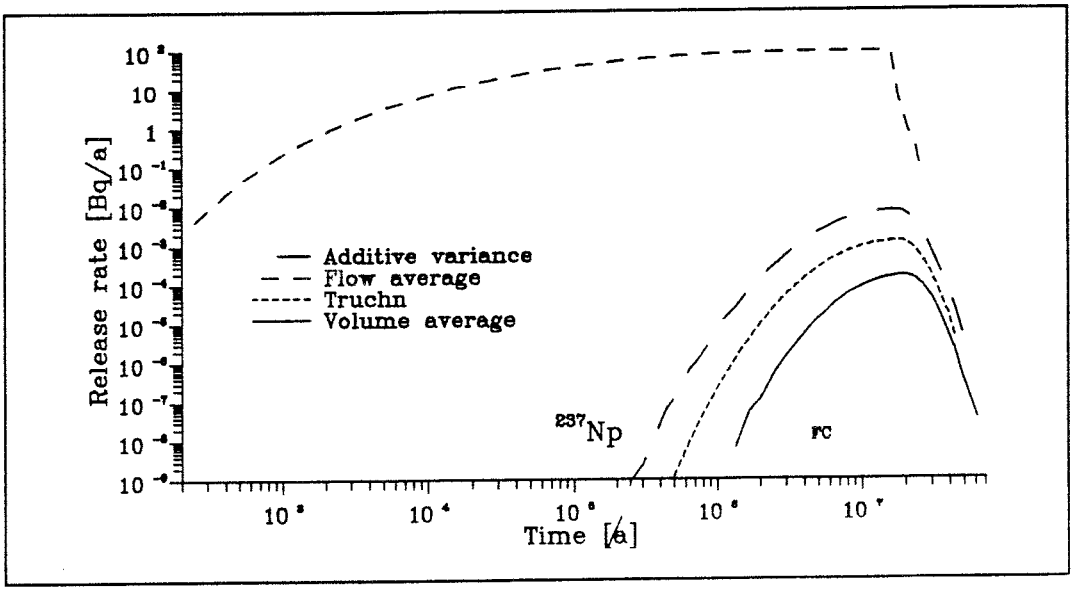

Figure 4.10 : Breakthrough for ^{237}Np using piecewise constant velocity.

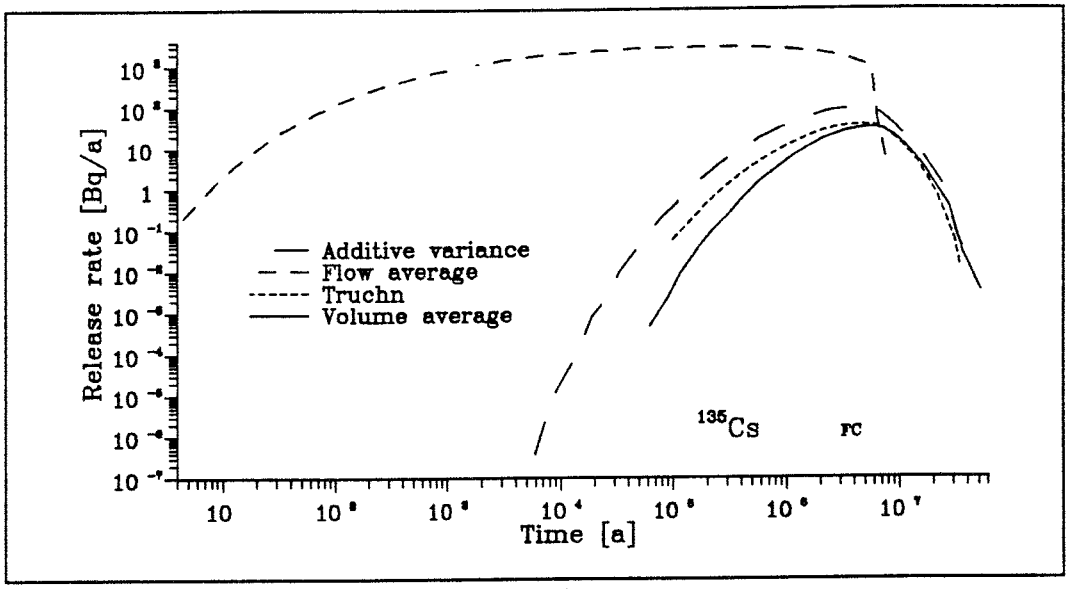

Figure 4.11 : Breakthrough for ^{135}Cs using piecewise constant velocity.

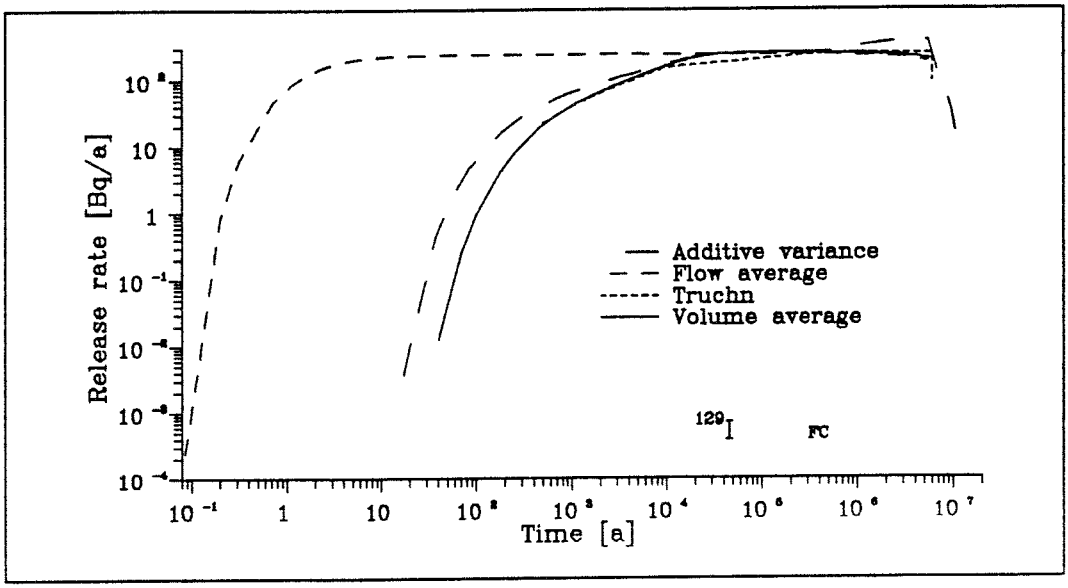

Figure 4.12 : Breakthrough for ^{129}I using piecewise constant velocity.

4.2.5 Sinusiodally varying velocity

The following values were used for the two average variations performed :

Flow average :	Pe = 2	$t_w = 131.76$
Additive variance :	Pe = 0.019	$t_w = 500$

The calculated breakthrough curves are shown in Figures 4.13 - 4.16. In Table 4.4 the time of the peak release, the peak release and the integrated release are given. The results given for volume average are identical to those shown in Section 4.2.2.

Table 4.4 : Summary of release data for sinusiodally varying velocity.

	Volume average	Flow average	Additive variance	TRUCHN
^{238}U				
Peak time	$2.29 \cdot 10^{10}$	$1.89 \cdot 10^{10}$	$1.19 \cdot 10^{10}$	$2.70 \cdot 10^{10}$
Peak release	$2.88 \cdot 10^{-2}$	$6.77 \cdot 10^{-2}$	$8.68 \cdot 10^{-2}$	$2.56 \cdot 10^{-2}$
Integrated release	$7.80 \cdot 10^{8}$	$1.85 \cdot 10^{9}$	$2.32 \cdot 10^{9}$	$6.99 \cdot 10^{8}$
^{237}Np				
Peak time	$1.94 \cdot 10^{7}$	$1.57 \cdot 10^{7}$	$1.56 \cdot 10^{7}$	$2.10 \cdot 10^{7}$
Peak release	$1.58 \cdot 10^{-4}$	$1.90 \cdot 10^{-1}$	$3.10 \cdot 10^{1}$	$1.33 \cdot 10^{-5}$
Integrated release	$2.77 \cdot 10^{3}$	$3.12 \cdot 10^{6}$	$4.98 \cdot 10^{8}$	$2.67 \cdot 10^{2}$
^{135}Cs				
Peak time	$5.31 \cdot 10^{6}$	$2.89 \cdot 10^{6}$	$6.11 \cdot 10^{5}$	$1.70 \cdot 10^{7}$
Peak release	$3.03 \cdot 10^{1}$	$3.45 \cdot 10^{2}$	$1.59 \cdot 10^{3}$	$1.09 \cdot 10^{1}$
Integrated release	$2.68 \cdot 10^{8}$	$2.43 \cdot 10^{9}$	$7.33 \cdot 10^{9}$	$2.14 \cdot 10^{8}$
^{129}I				
Peak time	$1.56 \cdot 10^{5}$	$3.27 \cdot 10^{4}$	$6.73 \cdot 10^{4}$	$6.80 \cdot 10^{3}$
Peak release	$2.56 \cdot 10^{2}$	$2.52 \cdot 10^{2}$	$2.43 \cdot 10^{2}$	$1.34 \cdot 10^{2}$
Integrated release	$1.28 \cdot 10^{9}$	$1.24 \cdot 10^{9}$	$1.20 \cdot 10^{9}$	$4.88 \cdot 10^{5}$

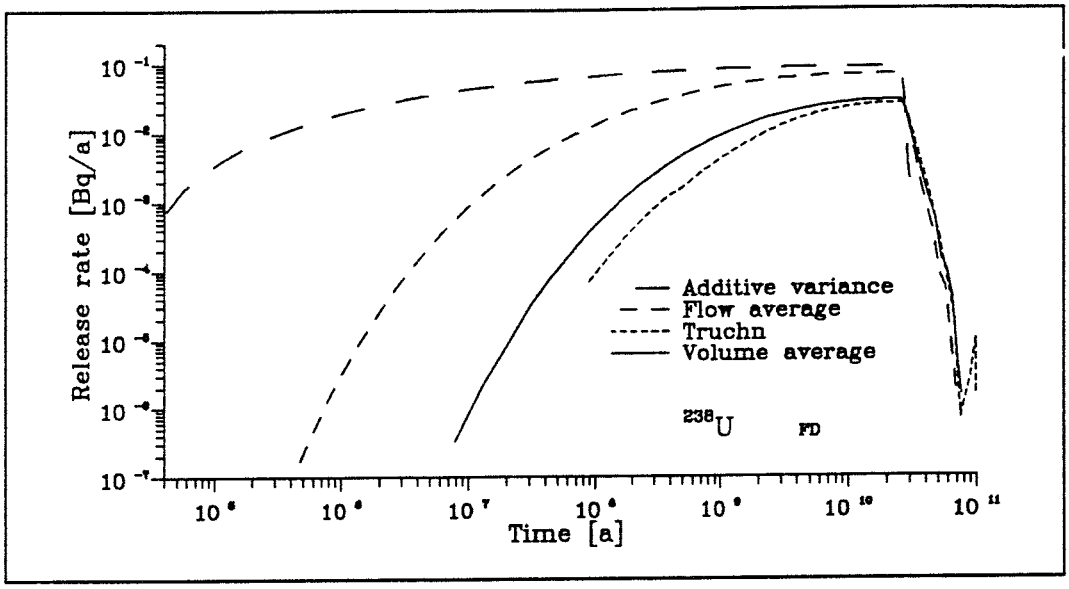

Figure 4.13 : Breakthrough for ^{238}U using sinusiodally varying velocity.

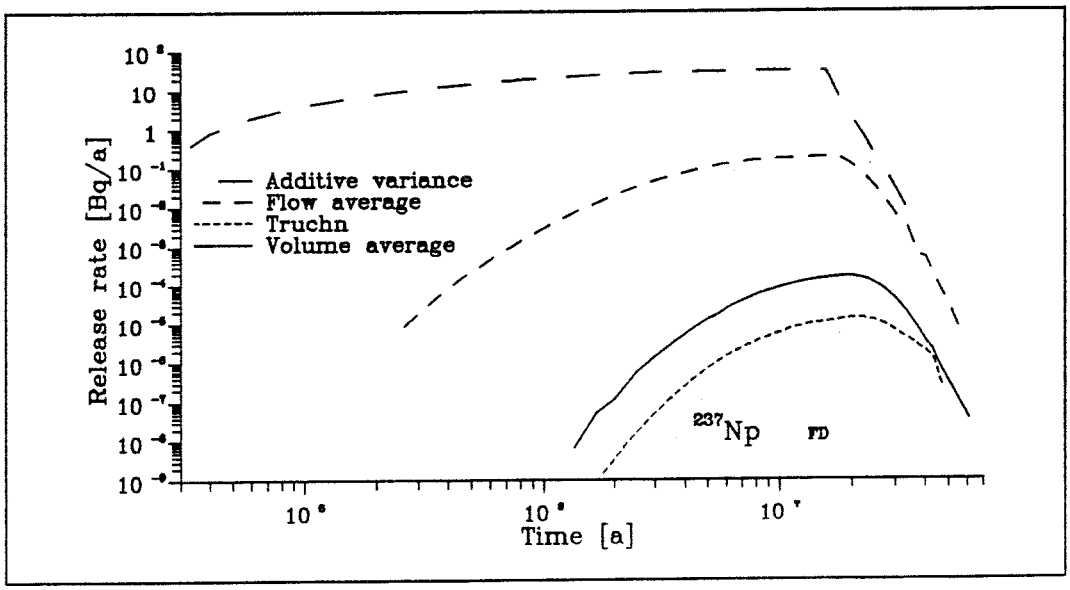

Figure 4.14 : Breakthrough for ^{237}Np using sinusiodally varying velocity.

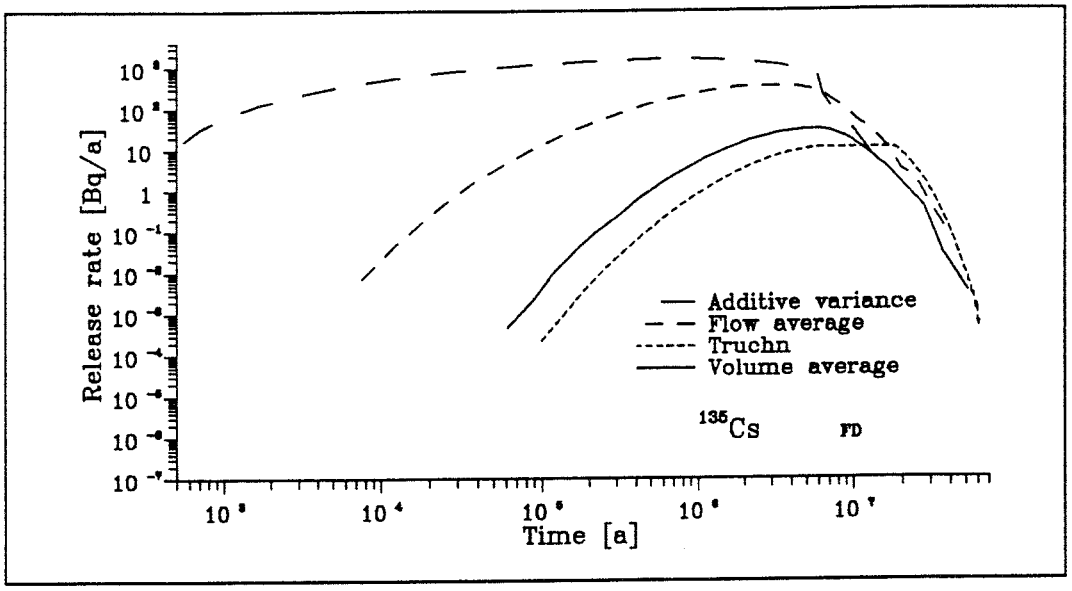

Figure 4.15 : Breakthrough for ^{135}Cs using sinusiodally varying velocity.

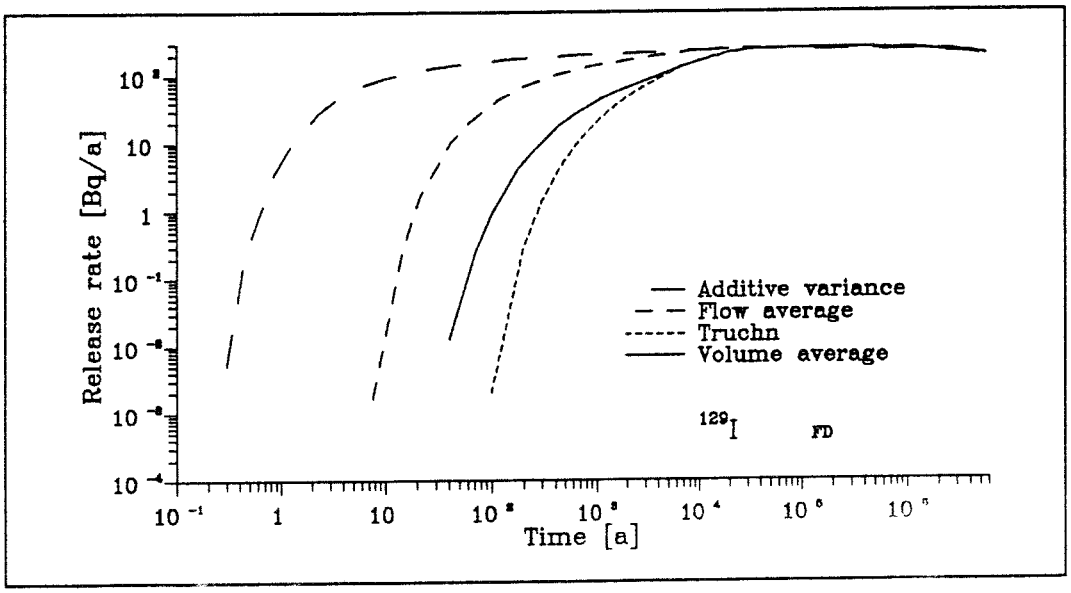

Figure 4.16 : Breakthrough for ^{129}I using sinusiodally varying velocity.

4.2.6 The Finnsjö test case

The following values were used for the two average variations performed :

Volume average :	Pe = 2	$t_w = 3126$
Flow average :	Pe = 2	$t_w = 7.71$
Additive variance :	Pe = 0.78	$t_w = 500$

The calculated breakthrough curves are shown in Figures 4.17 - 4.20. In Table 4.5 the time of the peak release, the peak release and the integrated release are given.

Table 4.5 : Summary of release data for the finnsjö test case.

	Volume average	Flow average	Additive variance	TRUCHN
^{238}U				
Peak time	$2.76 \cdot 10^{10}$	$5.73 \cdot 10^{9}$	$2.58 \cdot 10^{10}$	$3.00 \cdot 10^{10}$
Peak release	$1.37 \cdot 10^{-3}$	$1.04 \cdot 10^{-1}$	$5.85 \cdot 10^{-3}$	$1.40 \cdot 10^{-4}$
Integrated release	$3.89 \cdot 10^{7}$	$2.78 \cdot 10^{9}$	$1.62 \cdot 10^{8}$	$4.85 \cdot 10^{6}$
^{237}Np				
Peak time	$3.46 \cdot 10^{7}$	$1.28 \cdot 10^{7}$	$2.40 \cdot 10^{7}$	$5.10 \cdot 10^{7}$
Peak release	$4.46 \cdot 10^{-14}$	$4.54 \cdot 10^{1}$	$2.29 \cdot 10^{-8}$	$7.77 \cdot 10^{-23}$
Integrated release	$1.02 \cdot 10^{-6}$	$7.24 \cdot 10^{8}$	$4.51 \cdot 10^{-1}$	$1.93 \cdot 10^{-15}$
^{135}Cs				
Peak time	$1.29 \cdot 10^{7}$	$5.64 \cdot 10^{5}$	$7.69 \cdot 10^{6}$	$2.00 \cdot 10^{7}$
Peak release	$1.87 \cdot 10^{-2}$	$2.31 \cdot 10^{3}$	1.03	$2.02 \cdot 10^{-5}$
Integrated release	$2.60 \cdot 10^{5}$	$9.98 \cdot 10^{9}$	$1.14 \cdot 10^{7}$	$3.88 \cdot 10^{2}$
^{129}I				
Peak time	$4.90 \cdot 10^{5}$	$1.11 \cdot 10^{4}$	$4.36 \cdot 10^{5}$	$2.99 \cdot 10^{5}$
Peak release	$2.45 \cdot 10^{2}$	$2.51 \cdot 10^{2}$	$2.48 \cdot 10^{2}$	$2.46 \cdot 10^{2}$
Integrated release	$1.30 \cdot 10^{9}$	$1.22 \cdot 10^{9}$	$1.33 \cdot 10^{9}$	$1.32 \cdot 10^{9}$

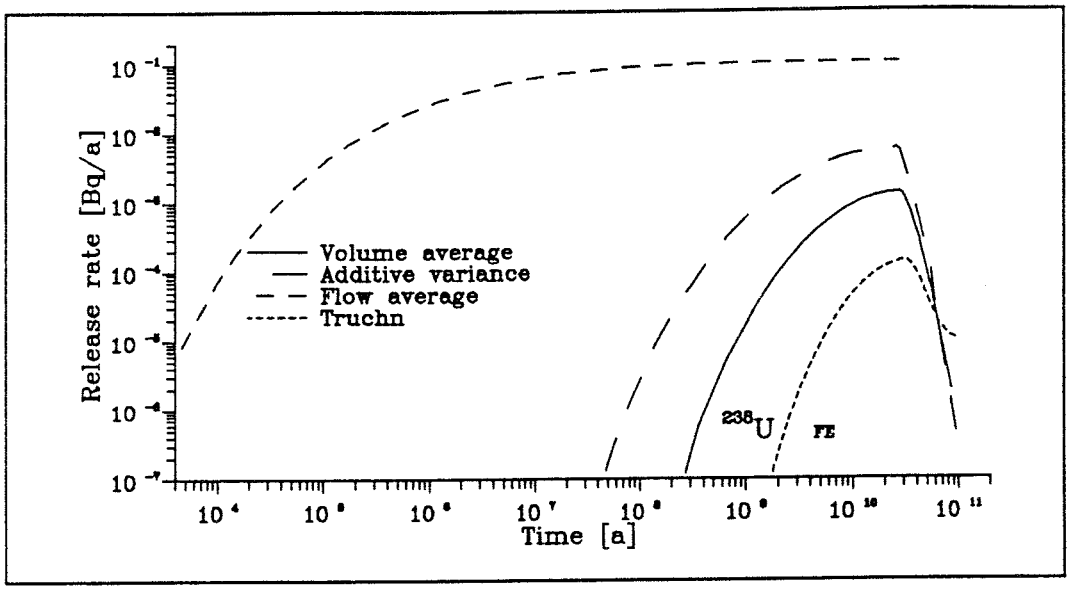

Figure 4.17 : Breakthrough for ^{238}U for the Finnsjö test case.

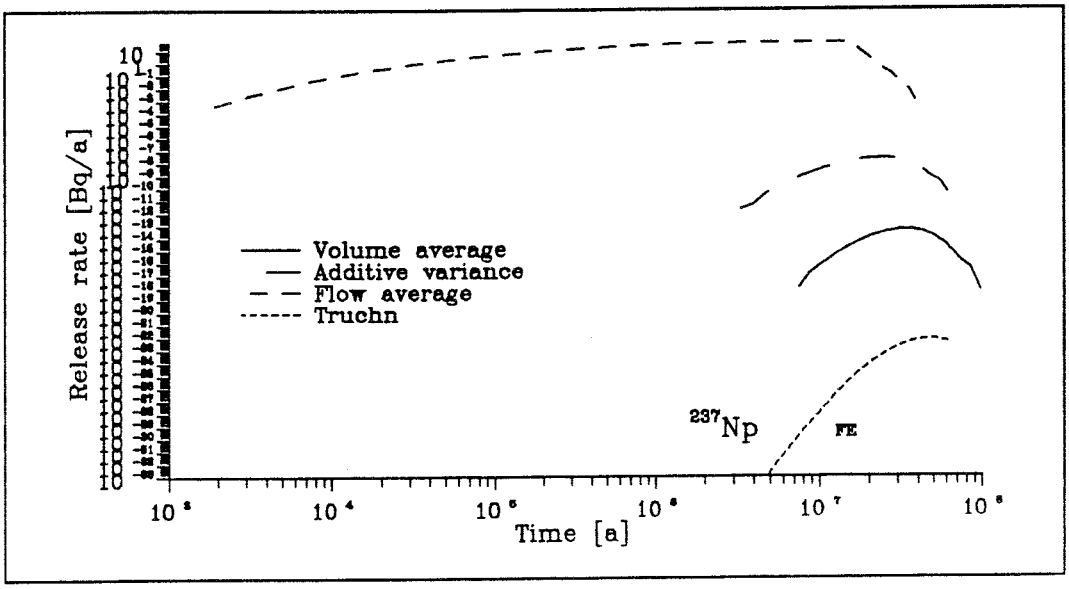

Figure 4.18 : Breakthrough for ^{237}Np for the Finnsjö test case.

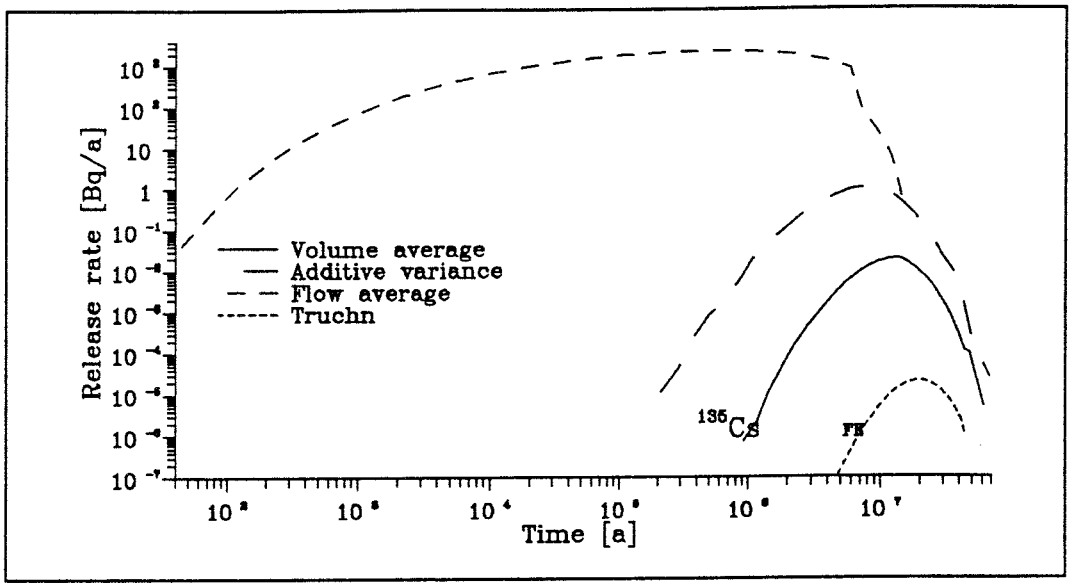

Figure 4.19 : *Breakthrough for ^{135}Cs for the Finnsjö test case.*

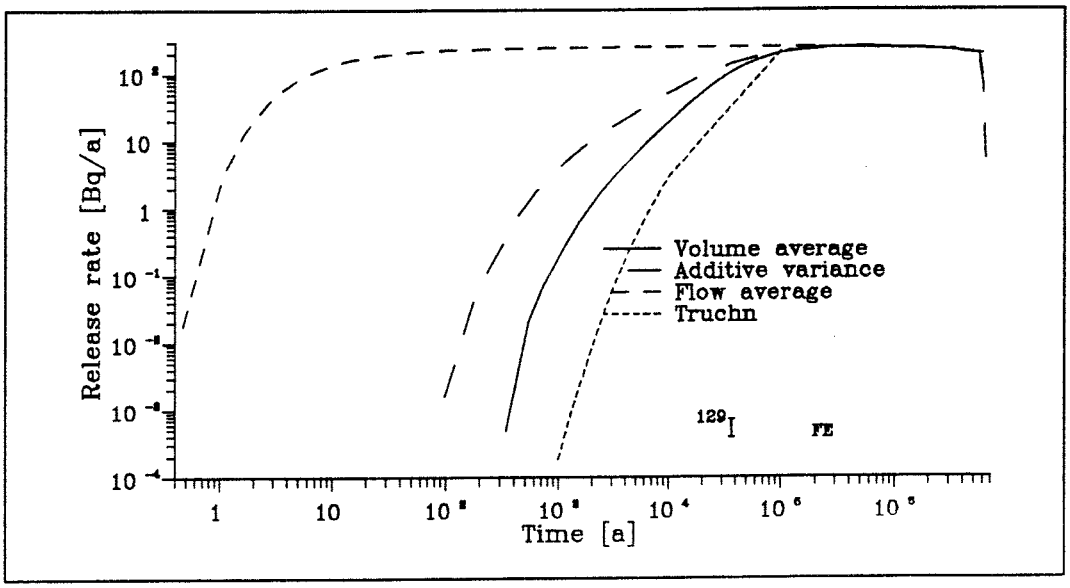

Figure 4.20 : *Breakthrough for ^{129}I for the Finnsjö test case.*

4.3 THE INFLUENCE OF A DIFFERENT Pe NUMBER ASSUMTION

In all cases described in the sections above the estimated Peclet number has been set to 2. This is value lies in the range used in previous studies of radionuclide migration, e.g. the KBS-3 study *[KBS-3, 1983]*. In order to study the effect of the magnitude of the dispersion on the agreement between the TRUCHN and the FARF31 calculations, the linear test case was run for ^{237}Np with the prior estimate of P_e set to 5.

The following values were used for the three average velocity variations performed :

Flow average :	Pe = 5	$t_w = 500$
Volume average :	Pe = 5	$t_w = 109.65$
Additive variance :	Pe = 0.045	$t_w = 500$

The breakthrough curves are shown in Figure 4.21 and some numeric results in Table 4.6. The breakthrough curves for $P_e = 2$ are given in Figure 4.22 in order to facilitate comparision. It can be concluded that there is no significant influence from the Peclet number on the agreement in the range tested.

Table 4.6 : *Summary of release data for linearily varying velocity with Pe = 5 and Pe = 2 for ^{237}Np.*

	Volume average	Flow average	Additive variance	TRUCHN
^{237}Np (Pe=5)				
Peak time	$2.44 \cdot 10^{7}$	$1.71 \cdot 10^{7}$	$1.52 \cdot 10^{7}$	$2.00 \cdot 10^{7}$
Peak release	$1.26 \cdot 10^{-7}$	$2.49 \cdot 10^{-2}$	$1.49 \cdot 10^{1}$	$3.57 \cdot 10^{-5}$
Integrated release	2.47	$4.16 \cdot 10^{5}$	$2.41 \cdot 10^{8}$	$6.37 \cdot 10^{2}$
^{237}Np (Pe=2)				
Peak time	$1.94 \cdot 10^{7}$	$1.65 \cdot 10^{7}$	$1.55 \cdot 10^{7}$	$1.90 \cdot 10^{7}$
Peak release	$1.58 \cdot 10^{-4}$	$3.65 \cdot 10^{-1}$	$3.16 \cdot 10^{1}$	$6.62 \cdot 10^{-4}$
Integrated release	$2.77 \cdot 10^{3}$	$5.95 \cdot 10^{6}$	$5.08 \cdot 10^{8}$	$1.13 \cdot 10^{4}$

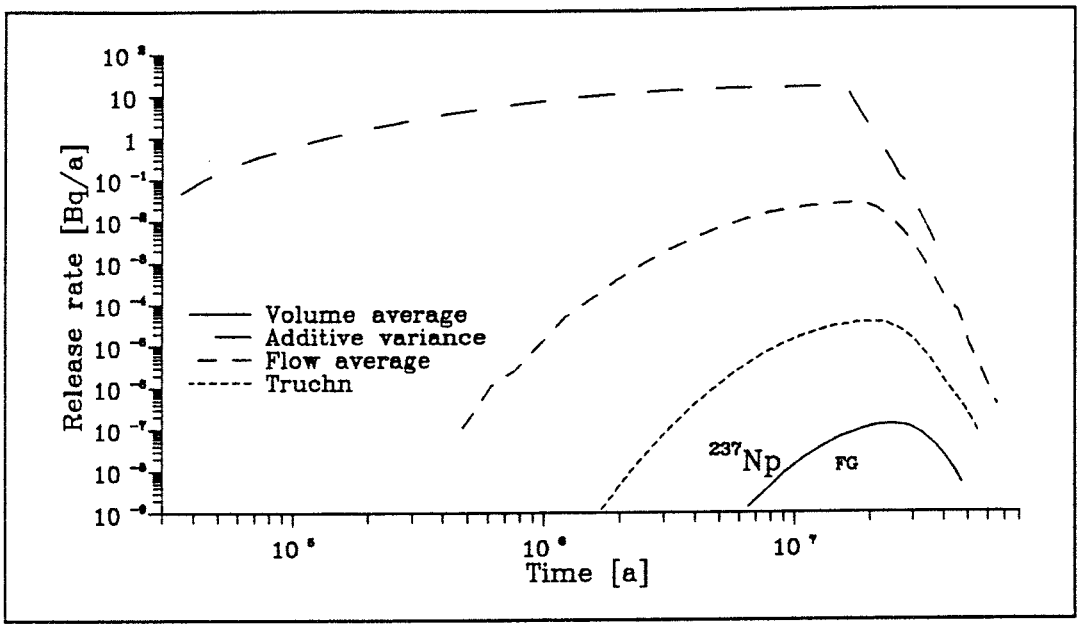

Figure 4.21 : Breakthrough curves for ^{237}Np using the linear velocity variation and Pe=5.

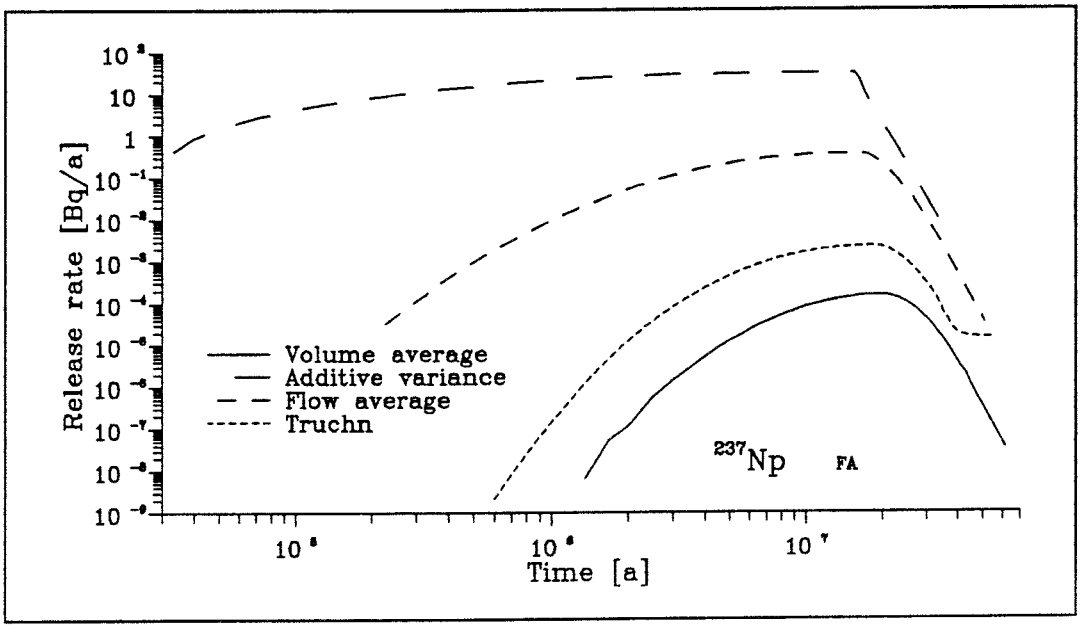

Figure 4.22 : Breakthrough curves for ^{237}Np using the linear velocity variation and Pe=2.

5 CONCLUSIONS

The peak release rate is well simulated by the Volume-Average model when the transport time is short compared to the half-life of the radionuclide. In these cases the peak releases are completely governed by the advective term. For the cases in which the dispersive transport plays a significant role, i.e. for the radionuclides that decay significantly so that the leading edge of the plume determines the peak level, the agreement between the numerical and the analytical solutions, however, is significantly poorer. In particular, the agreement for the particle track from Finnsjön is very poor because of the long transport times.

In the cases where low velocities predominate, the Additive-Variance model yields a too low Peclet number leading to an extremely early arrival of the radionuclide. This is the case in the cases with linearly increasing velocity (A) and sinusoidal velocity variation (D). In the other cases the Flow-Average model yields the earliest arrival. It is evident from the results that the bias for the high-velocity part caused in the Flow-Average model creates unreasonably high average velocities. In particular this is the case when high velocities predominate (exponentially increasing velocity, case B, and piecewise constant velocity, case C). This model can therefore be conclusively ruled out.

In the numerical calculations the dispersion coefficient has been assumed to be proportional to the velocity. This concept was chosen because it gives a behaviour of the system which is consistent with the expected behaviour of a fracture network. It should be pointed out that there are no evaluated evidence from field experiments that support a particular concept for the dispersion coefficient's dependence of the velocity. In the analytical solutions the velocity is constant. It is therefore not possible to distinguish between a constant dispersion length (as in the numerical calculations) and a constant dispersion coefficient in this context.

In conclusion, it seems difficult, if not impossible, to find an averaging model which, starting from a particle track and the velocity variation along it, will give good a priori estimates of both the advective transport and the dispersion. This is especially true when the Peclet number is so low as is predicted by field experiments (Pe = 1-10). The Peclet numbers obtained with the different models tested in this study all fall within a range of two orders of magnitude. This range is not extremely large compared to the variability of the Peclet numbers obtained in field measurements.

REFERENCES

B. Allard, F.Karlsson, I.Neretnieks, Concentration of particulate matter and humic substanses in deep groundwaters and estimated effects on the adsorption and transport of radionuclides., Not yet published.

A. Bengtsson, 1990, " PRETRU - A preprocessor for TRUCHN far field migration calculations." **SKB AR 90-22**, Swedish Nuclear Fuel and Waste Management Co., Stockholm, Sweden

B. Lindbom, A.Boghammar, H.Lindberg, J.Bjelkås, 1991, "Numerical groundwater flow calculations at the Finnsjö site.", **SKB TR 91-12**, Swedish Nuclear Fuel and Waste Management Co., Stockholm, Sweden

I. Neretnieks, A.Rasmuson, "An approach to modelling radionuclide migration in a medium with strongly varying velocity and block sizes along the flow path.", **Wat.Resour.Res.**, Vol20 (12), p1823ff, 1984

S. Norman, N.Kjellbert, 1990, "FARF31 - A far field radionuclide migration code for use with the PROPER package.", **SKB TR 90-01**, Swedish Nuclear Fuel and Waste Management Co., Stockholm, Sweden

A. Rasmuson, A.Bengtsson, B.Grundfelt, I.Neretnieks, 1982, "Radionuclide chain migration in fissured rock - The influence of matrix diffusion.", **KBS TR 82-04**, Swedish Nuclear Fuel and Waste Management Co., Stockholm, Sweden

Kärnbränslecykelns slutsteg. Använt kärnbränsle - KBS-3., Svensk Kärnbränsleförsörjning AB, Stockholm, 1983

NOTATION

ε_f	Flow porosity	[]
ε_p	Porosity of rock matrix	[]
λ_i	Decay constant for nuclide i	[1/s]
ρ_f	Fluid density	[kg/m^3]
ρ_p	Host rock density	[kg/m^3]
a	Surface are per unit volume of mobile liquid	[1/m]
2b	Fracture apperture	[m]
c_i	Concentration of nuclide i in mobile water	[moles/m^3]
$c_{p,i}$	Concentration of nuclide i in the rock matrix	[moles/m^3]
D	Dispersion coefficient	[m^2/s]
D_a	Apparent diffusion coefficient	[m^2/s]
D_e	Effictive diffusion coefficient	[m^2/s]
D_L	Longitudal dispersion coefficient	[m^2/s]
L	Streamtube length	[m]
P_e	Peclet number	[]
R_i	Effective matrix sorption retention factor	[]
S	Fracture spacing	[m]
t	Time	[s]
t_w	Residence time	[s]
u	Groundwater velocity	[m/s]
u_0	Groundwater Darcy velocity	[m/s]
w	Term describing the capacity between fracture transport and matrix diffusion	[moles/m^3/s]
x	Distance into rock matrix	[m]
z	Distance along the flow tube	[m]

Superscripts :

-	Average
*	Estimated (Used in the calculations)

APPENDIX A

Quality Assurance

Files created and processed during the project

1 FARF31 files

Files created and used on the SKB Convex C210 machine for use by FARF31 were stored on directory **/files/home/users/kemanb/0215** and it's subdirectories.

The following naming convention has been used :

Name : Defines type of problem.

Template - **FXYZZZZZ** where :

X : define type of velocity variation
- \- Constant velocity
- A Linear variation
- B Exponentially increasing
- C Piecewise constant
- D Sinusoidally varying
- E Finnsjö particle track number 4
- G Linear with Pe=5

Y : define type of averaging used
- 0 TRUCHN results
- 1 Volume average
- 2 Additive variance
- 3 Flow average

ZZZZZ : type of nuclide ^{238}U, ^{237}Np, ^{135}Cs or ^{129}I

Extension :

The extension defines the type of file. The following extensions have been used :

TSIN : Input migration rate [mol/a] for all nuclides. The name part of the filename only consists of FXY since the file hold information on all nuclides. The same file has been used for all variations performed, hence only the file **fa1.tsin** has been stored on tape.

TSOUT : Output migration rate [mol/a] for all nuclides. The name part of the filename only consists of FXY since the file hold information on all nuclides.

PARAMETERS : Physical data and problem specific data. Name part only consist of FXY

CHAINS : Nuclide data for all nuclides. The name part of the filename only consists of FXY since the file hold information on all nuclides. The same nuclide chains have been used for all variations performed, hence only the file **fa1.chains** has been stored on tape.

DAT : Output migration rate [Bq/a] for one nuclide.

PEAK : Peak release rate [Bq/a] and time [a] and integrated release [Bq] for all nuclides.

The following utility programs have been stored, they did all reside in subdirectory **farf31** :

FARFGO : Shell-script to handle all the utility programs.

PREFARF : FORTRAN program to preprocess and setup the PARAMETERS and CHAINS file for a specific problem. It uses to database files stored on subdirectory **inbase**, called **nucbase** and **rockbase.**

POSTFARF : FORTRAN program to postprocess the TSOUT file and calc e the output in Bq/a.

CUTTSACT : FORTRAN program to cut the output file from POSTFARF into one file for each nuclide.

PEAK : FORTRAN program to calculate the peak release and integrated release.

Example of file flow for case FA1 :

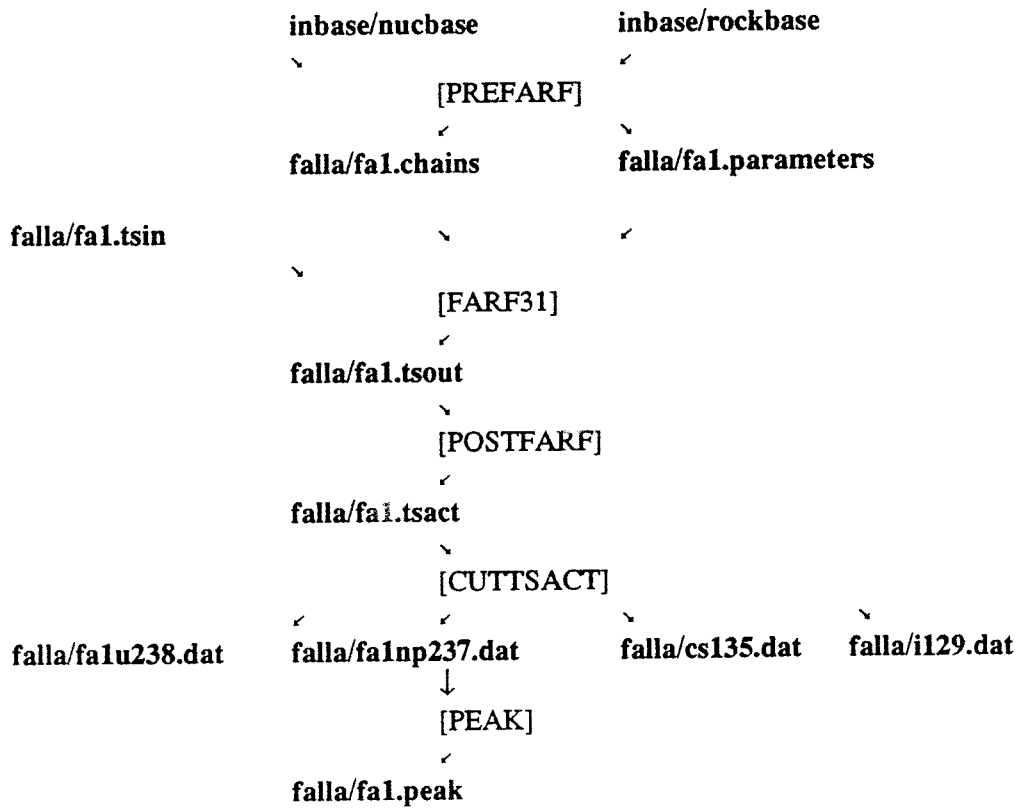

2 TRUCHN files

Files created and used on the SKB Convex C210 computer for the numerical reference calculations were stored on the directory **/files/home/users/kemab/0215**. Under this directory is six subdirectories, one for each of the stream tube scenarios. **/const, /linear, /exp, /piece, /sinus** and **/ban4**. Under each of them is one subdirectory for each of the four different nuclides: **/i129, /cs137, /np237** and **/u238**. In most cases the discretisation and initial creation of an incomplete TRUCHN input data file through PRETRU is done on the stream tube directory level. The preliminary TRUCHN input data file is then transferred to the correct nuclide subdirectory, edited, given a serial number and run.

The file naming conventions are quite simple. There are three groups of files: Data files common to the whole project, data files describing each of the flow tube scenarios and the input- and output files for a particular TRUCHN run.

The data files common to the whole project are three files
- **0215.bod** which describes the geometry of the diffusion into the rock matrix.
- **0215.mat** which contains the nuclide specific migration parameters and
- **0215.sor** which contains the mass sorption coefficients for the different nuclides.

Multiple identical copies exists of these PRETRU input files as they have to be on the current directory when PRETRU is run.

The stream tube input data files exist at least as one copy on each stream tube directory and they are called banax.tub where :

x=a	Linearily increasing velocity
x=b	exponentially increasing velocity
x=c	Piecewise constant velocity
x=d	Sinusoidally varying velocity
x=e	Lake Finnsjon simulation stream tube and
x=f	Constant velocity.

The same discretisation is used for all four nuclides for a particular stream tube scenario. A compact description of the node positions and lengths is written in the file NODFIL which also resides one on each of the stream tube root directories.

The files for a particular TRUCHN run all reside on the nuclide subdirectory level. All the files have the same name except for the extension which is

.inp	TRUCHN input data file
.out	TRUCHN main output data file.
.dmp	Concentrations in all nodes at the end of a calculation.
.pul	Nuclide fluxes at the outer boundaries at the printout intervals.
.tru	Concentration values of the two fracture nodes on each side of the observation point.
.dat	Nuclide flux past the observation point
.run	Diagnostic logging of the TRUCHN and post processing program runs.

The name of the .inp-file automatically determines the name of the others.

As an example the complete chain of events is shown for run 1 of Cs-135 and the constant velocity stream tube scenario. (See figure on the following side)

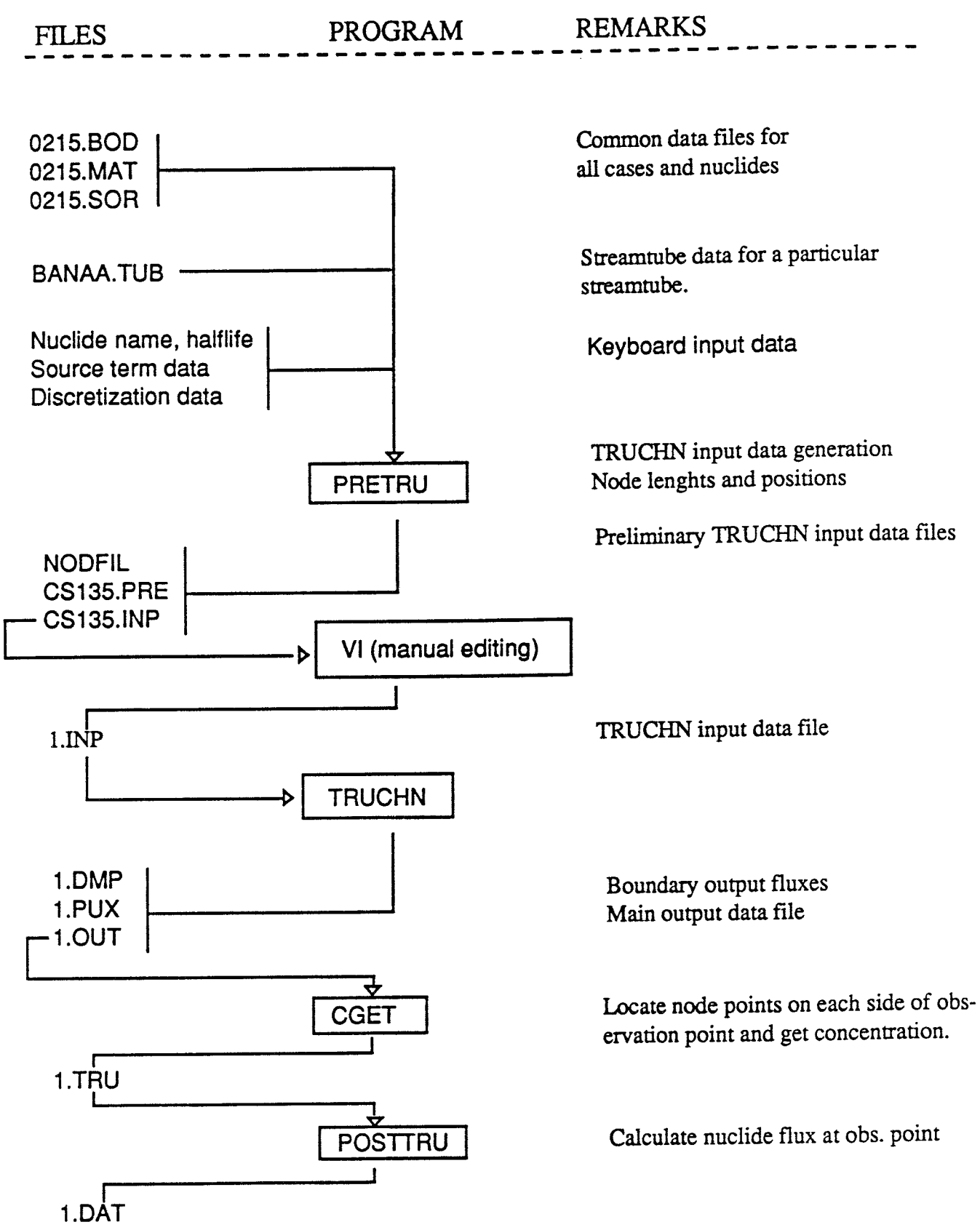
FILES
PROGRAM
REMARKS
0215.BOD
0215.MAT
0215.SOR
Common data files for all cases and nuclides
BANAA.TUB
Streamtube data for a particular streamtube.
Nuclide name, halflife
Source term data
Discretization data
Keyboard input data
PRETRU
TRUCHN input data generation
Node lenghts and positions
Preliminary TRUCHN input data files
NODFIL
CS135.PRE
CS135.INP
VI (manual editing)
1.INP
TRUCHN input data file
TRUCHN
1.DMP
1.PUX
1.OUT
Boundary output fluxes
Main output data file
CGET
Locate node points on each side of obs-ervation point and get concentration.
1.TRU
POSTTRU
Calculate nuclide flux at obs. point
1.DAT

List of SKB reports

Annual Reports

1977-78
TR 121
KBS Technical Reports 1 – 120
Summaries
Stockholm, May 1979

1979
TR 79-28
The KBS Annual Report 1979
KBS Technical Reports 79-01 – 79-27
Summaries
Stockholm, March 1980

1980
TR 80-26
The KBS Annual Report 1980
KBS Technical Reports 80-01 – 80-25
Summaries
Stockholm, March 1981

1981
TR 81-17
The KBS Annual Report 1981
KBS Technical Reports 81-01 – 81-16
Summaries
Stockholm, April 1982

1982
TR 82-28
The KBS Annual Report 1982
KBS Technical Reports 82-01 – 82-27
Summaries
Stockholm, July 1983

1983
TR 83-77
The KBS Annual Report 1983
KBS Technical Reports 83-01 – 83-76
Summaries
Stockholm, June 1984

1984
TR 85-01
Annual Research and Development Report 1984
Including Summaries of Technical Reports Issued during 1984. (Technical Reports 84-01 – 84-19)
Stockholm, June 1985

1985
TR 85-20
Annual Research and Development Report 1985
Including Summaries of Technical Reports Issued during 1985. (Technical Reports 85-01 – 85-19)
Stockholm, May 1986

1986
TR 86-31
SKB Annual Report 1986
Including Summaries of Technical Reports Issued during 1986
Stockholm, May 1987

1987
TR 87-33
SKB Annual Report 1987
Including Summaries of Technical Reports Issued during 1987
Stockholm, May 1988

1988
TR 88-32
SKB Annual Report 1988
Including Summaries of Technical Reports Issued during 1988
Stockholm, May 1989

1989
TR 89-40
SKB Annual Report 1989
Including Summaries of Technical Reports Issued during 1989
Stockholm, May 1990

Technical Reports

List of SKB Technical Reports 1991

TR 91-01
Description of geological data in SKB's database GEOTAB
Version 2
Stefan Sehlstedt, Tomas Stark
SGAB, Luleå
January 1991

TR 91-02
Description of geophysical data in SKB database GEOTAB
Version 2
Stefan Sehlstedt
SGAB, Luleå
January 1991

TR 91-03
1. The application of PIE techniques to the study of the corrosion of spent oxide fuel in deep-rock ground waters
2. Spent fuel degradation
R S Forsyth
Studsvik Nuclear
January 1991

TR 91-04
Plutonium solubilities
I Puigdomènech[1], J Bruno[2]
[1]Enviromental Services, Studsvik Nuclear, Nyköping, Sweden
[2]MBT Tecnologia Ambiental, CENT, Cerdanyola, Spain
February 1991

TR 91-05
Description of tracer data in the SKB database GEOTAB
SGAB, Luleå
April, 1991

TR 91-06
Description of background data in the SKB database GEOTAB Version 2
Ebbe Eriksson, Stefan Sehlstedt
SGAB, Luleå
March 1991

TR 91-07
Description of hydrogeological data in the SKB's database GEOTAB Version 2
Margareta Gerlach[1], Bengt Gentzschein[2]
[1]SGAB, Luleå
[2]SGAB, Uppsala
April 1991

TR 91-08
Overview of geologic and geohydrologic conditions at the Finnsjön site and its surroundings
Kaj Ahlbom[1], Sven Tirén[2]
[1]Conterra AB
[2]Sveriges Geologiska AB
January 1991

TR 91-09
Long term sampling and measuring program. Joint report for 1987, 1988 and 1989. Within the project: Fallout studies in the Gideå and Finnsjö areas after the Chernobyl accident in 1986
Thomas Ittner
SGAB, Uppsala
December 1990

TR 91-10
Sealing of rock joints by induced calcite precipitation. A case study from Bergeforsen hydro power plant
Eva Hakami[1], Anders Ekstav[2], Ulf Qvarfort[2]
[1]Vattenfall HydroPower AB
[2]Golder Geosystem AB
January 1991

TR 91-11
Impact from the disturbed zone on nuclide migration – a radioactive waste repository study
Akke Bengtsson[1], Bertil Grundfelt[1], Anders Markström[1], Anders Rasmuson[2]
[1]KEMAKTA Konsult AB
[2]Chalmers Institute of Technology
January 1991

TR 91-12
Numerical groundwater flow calculations at the Finnsjön site
Björn Lindbom, Anders Boghammar, Hans Lindberg, Jan Bjelkås
KEMAKTA Consultants Co, Stockholm
February 1991

TR 91-13
Discrete fracture modelling of the Finnsjön rock mass Phase 1 feasibility study
J E Geier, C-L Axelsson
Golder Geosystem AB, Uppsala
March 1991

TR 91-14
Channel widths
Kai Palmqvist, Marianne Lindström
BERGAB-Berggeologiska Undersökningar AB
February 1991

TR 91-15
Uraninite alteration in an oxidizing environment and its relevance to the disposal of spent nuclear fuel
Robert Finch, Rodney Ewing
Department of Geology, University of New Mexico
December 1990

TR 91-16
Porosity, sorption and diffusivity data compiled for the SKB 91 study
Fredrik Brandberg, Kristina Skagius
Kemakta Consultants Co, Stockholm
April 1991

TR 91-17
Seismically deformed sediments in the Lansjärv area, Northern Sweden
Robert Lagerbäck
May 1991

TR 91-18
Numerical inversion of Laplace transforms using integration and convergence acceleration
Sven-Åke Gustafson
Rogaland University, Stavanger, Norway
May 1991

TR 91-19
NEAR21 - A near field radionuclide migration code for use with the PROPER package
Sven Norman[1], Nils Kjellbert[2]
[1]Starprog AB
[2]SKB AB
April 1991

TR 91-20
Äspö Hard Rock Laboratory. Overview of the investigations 1986-1990
R Stanfors, M Erlström, I Markström
June 1991

TR 91-21
Äspö Hard Rock Laboratory. Field investigation methodology and instruments used in the pre-investigation phase, 1986-1990
K-E Almén, O Zellman
June 1991

TR 91-22
Äspö Hard Rock Laboratory. Evaluation and conceptual modelling based on the pre-investigations 1986-1990
P Wikberg, G Gustafson, I Rhén, R Stanfors
June 1991

TR 91-23
Äspö Hard Rock Laboratory. Predictions prior to excavation and the process of their validation
Gunnar Gustafson, Magnus Liedholm, Ingvar Rhén, Roy Stanfors, Peter Wikberg
June 1991

TR 91-24
Hydrogeological conditions in the Finnsjön area. Compilation of data and conceptual model
Jan-Erik Andersson, Rune Nordqvist, Göran Nyberg, John Smellie, Sven Tirén
February 1991

TR 91-25
The role of the disturbed rock zone in radioactive waste repository safety and performance assessment. A topical discussion and international overview.
Anders Winberg
June 1991